“The Effect of Interlayer Distance and Doping on the Performance of Multilayer Graphene Nano Ribbons as VLSI Interconnects”

A Thesis Submitted in Partial Fulfillment of the Requirement for the Award of the Degree of

Master of Technology

In

VLSI Design

Submitted By:

Kashish Wadhwa

Roll No. 601562014

Under Supervision of

Dr. Karmjit Singh Sandha

(Assistant Professor, ECED)

ELECTRONICS AND COMMUNICATION ENGINEERING DEPARTMENT

THAPAR UNIVERSITY, PATIALA, PUNJAB

JULY, 2017

DECLARATION

I, **Kashish Wadhwa** hereby declare that the work presented in this thesis entitled **"The Effect of Interlayer Distance and Doping on the Performance of Multilayer Graphene Nano Ribbons as VLSI Interconnects "** in partial fulfillment of the requirement for the award of degree of Master of Technology in VLSI Design submitted at electronics and Communication Engineering Department, Thapar University, Patiala is an authentic record of my own work carried out by me under supervision of **Dr. Karmjit Singh Sandha** (Assistant Professor, ECED) during 2015-2017. The matter presented in this has not been submitted either in part or full to any other university or institute for the award of any other degree.

Date 21-8-17

Kashish Wadhwa
Roll No. 601562014

It is certified that the above statement made by the candidate is correct to the best of my knowledge and belief.

Date 21-8-17

Dr. Karmjit Singh Sandha
Assistant Professor
ECED, Thapar University
Patiala

ACKNOWLEDGEMENT

This report has only been possible with the constant guidance and expertise of Dr. Karmjit Singh Sandha, Assistant Professor, Electronics and Communication Engineering Department, Thapar University, Patiala and I would like to take this opportunity to express my sincere gratitude to him.

I am also thankful to Dr. Alpana Agarwal, Head of ECE Department, for providing us the adequate infrastructure for carrying out the work.

I am also thankful to Dr. Hem Dutt Joshi, PG Coordinator as well as Dr. Anil Arora, Program Coordinator and the entire faculty and staff of Electronics and Communication Engineering Department for th**e** motivation and inspiration that triggered me for the work.

I would also like to thank my friends who always motivated me and have more or less contributed to the preparation of this report. I will be always indebted to them.

Last but not the least, I would like to thank my parents for their years of unyielding love and encourage. They have always wanted the best for me and I admire their determination and sacrifice.

Kashish Wadhwa

ABSTRACT

Graphene nanoribbons are considered as a potential VLSI interconnect material. Performance of deep sub micron circuits is deeply impacted by the interconnect due to reduced pitch size. The impact of interlayer distance on the performance in terms of propagation delay, power dissipation and power delay product (PDP) of multilayer GNR interconnect material is studied. Propagation delay is estimated for different interconnect length as well by using ESC model for GNR interconnects. This analysis is performed on 16nm technology node. It is found that for a doped multilayer GNR VLSI interconnects, the approximate optimum interlayer distance is 0.575nm at which MLGNR provides the optimum delay, power and PDP, other than this value the delay, power dissipation and power delay product is in increasing order. The similar analysis is also performed on 22nm technology node and found the same optimum interlayer distance around 0.575nm. But the propagation delay, power dissipation and power delay product are reduced as compare to the 16nm technology node.

Impact of conductance of GNR interconnects is also studied. Resistance per unit length for different GNR versus interconnect cross-sectional width for interconnects length larger than its mean free path is also plotted. Further, the impact of fermi energy on propagation delay and power dissipation is studied for different technology nodes. As the scaling continues, the propagation delay and power dissipation of MLGNR interconnect increases. A suitable number of repeaters are inserted to obtain the performance analysis of GNR interconnect. The results so obtained show the performance of graphene nano ribbons with increased doping. Thus MLGNR with suitable Fermi energy has a potential to replace copper at global interconnect lengths.

TABLE OF CONTENTS

LIST OF ACRONYMS

GNR	Graphene Nano Ribbons
CNT	Carbon Nano Tube
MLGNR	Multi Layer Graphene Nano Ribbons
SLGNR	Single Layer Graphene Nano Ribbons
ESC	Equivalent single Conductor
VLSI	Very Large Scale Integration
DIL	Driver Interconnect Load
MFP	Mean Free Path
MWCNT	Multi Wall Carbon Nano Tube
SWCNT	Single Wall Carbon Nano Tube
PDP	Power Delay Product
ITRS	International Technology Roadmap for Semiconductors

LIST OF FIGURES

LIST OF TABLES

CHAPTER 1
INTRODUCTION

1.1 MOTIVATION

A VLSI interconnect is a thin film of conducting material which provides electrical connection between different nodes of the circuit. Blocks are electrically connected by the wires called interconnects [1]. Interconnects also provides power and clocks to all the blocks of ICs. There are three types of interconnects i.e. local, intermediate and global interconnects. Gates and Transistors are connected inside a functional block using the local interconnects. First two metal layers are of local interconnects and consists of few transistors. Intermediate transistors are longer and wider in size than local interconnects. For clock distribution within a length of 3-4nm, intermediate interconnects are used. Top few layers are of global interconnects which provides clock and power distribution [2]. Figure 1.1 shows the hierarchy of metal levels for distribution of interconnects [2]

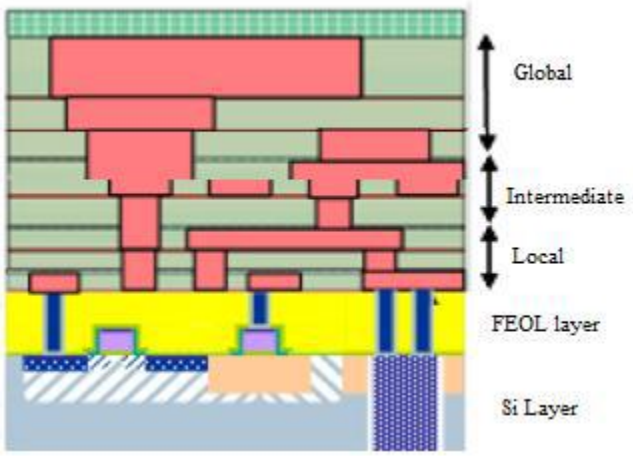

Figure 1.1 Hierarchy of metal levels for distribution of interconnects [2]

In a modern VLSI technology, it has become a complex task to connect the various components on a chip. The dimensions of the transistors are reducing due to the miniaturization of transistors [3]. Before copper, aluminum was used as a VLSI interconnects material because of good adherence and better conductivity with silicon. But due to high integration, electro migration occurs in aluminum. To overcome the electro migration problem, copper is used as interconnect material because copper has high current carrying density. Now- a-days, copper is the mostly used interconnect material. But in deep sub micron technology nodes, the copper resistance increases due to the surface roughness and grain boundary scattering. Due to this propagation delay and power dissipation increases. To

overcome this problem, carbon nano tubes (CNTs) and graphene nano ribbons (GNRs) are used as VLSI interconnect. Figure 1.2 shows the structure of copper interconnect, CNT-Bundle and multilayer GNR interconnect [3]

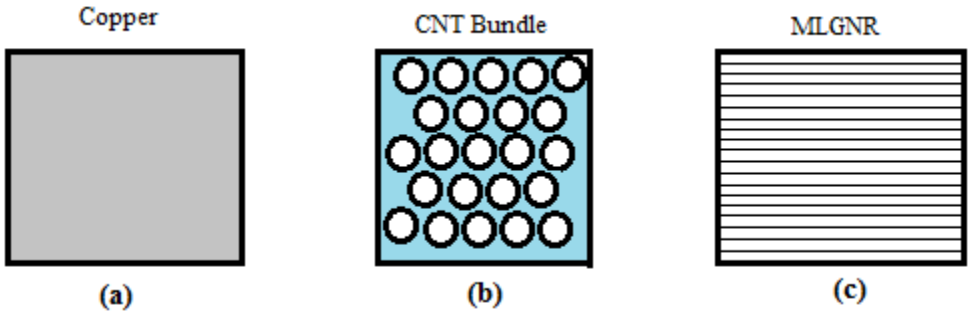

Figure 1.2 Structures a) Copper Interconnect b) CNT-Bundle c) MLGNR Interconnect [3]

GNRs and CNTs both have better electrical, mechanical and thermal properties in comparison to the copper. CNT is a graphene sheet rolled up in the form of hollow cylinder. GNR is a thin sheet of graphene patterned in a 2-D honeycomb lattice structure. There are two types of GNR namely armchair GNR and Zigzag GNR. The mean free path of graphene is longer than the copper. Both CNT and GNR have the potential to replace the copper as a VLSI interconnects.

1.2 INTRODUCTION OF COPPER INTERCONNECT

Earlier aluminum was the interconnect material. A onetime transition from aluminum to copper interconnects occurred in the industry. Due to increase in the feature size, the electro migration problem in aluminium is increased. To overcome this, the copper is used as a VLSI interconnects because of its lower resistivity. Due to low resistivity, the propagation delay and power dissipation decreases in integration circuits [4]. Switching of transistors between Vcc to ground determines the speed of integrated circuits. The propagation delay decides the speed of transistors. As the technology reduces, the transistor delay also reduces, but the propagation delay of interconnect not reduces at the same pace. Time constant of circuit determines the propagation delay of interconnect. Resistive and capacitive components decide the time constant of the circuit. We can reduce the RC time constant by decreasing the resistivity of the material or by using the material having low permittivity. Resistivity is decreased by 40% when copper is replaced by aluminium. So the decrease in the resistivity causes the decrease in the propagation delay and power dissipation. A proper suitable dielectric material also reduces the propagation delay. Thermal conductivity of copper is also better than aluminium. It is also proved that copper is 100 times immune to electro migration

in comparison to aluminium. In electro migration problem, the atoms are damaged due to large current density resulting in material breakdown. Copper is also good for the routing because the number of metal layers are reduced by using copper as material. Due to large scaling, the performance of copper reduces [5]. Due to the manufacturing of 2-D graphene sheets and good lithographic techniques, the graphene based interconnects replaces the copper interconnects.

1.3 GRAPHENE NANO RIBBON INTERCONNECTS

Introduction

Graphene is a flat 2D- single atomic layer sheet of carbon atoms. Recent researches show that GNR shows major interest in the electronic systems. GNRs are the unrolled CNTs having the same electronic properties as of carbon nano tubes. On the basis of geometry the graphene nano ribbons are classified as metallic and semiconducting graphene nano ribbons. The mean free path of the high quality graphenes is similar to the CNTs and has large current densities as of CNTs. The good advantage of GNRs over CNTs is the straight forward fabrication process [6].

The first isolation of graphene was through mechanical exfoliation of highly ordered pyrolytic graphite. This approach has proven very advantageous for research purposes and discoveries. Thermal decomposition is the method towards wafer level preparation of graphene. In this approach the flat surfaces of SiC wafer are heated in a vacuum to temperature above 1250^0C. In this process, the ultrathin graphene films are obtained whose thickness is determined by temperature. Although the production of multi layer graphene is also done having same properties as of isolated single layer graphene sheets. The preparation of graphene by wafer level methods, still lack the grain size and uniformity needed in large scale integration of graphene devices. Top down lithography is also used to pattern GNRs and to make interconnects and devices in a good way. Depending on the geometry, the metallic or semiconducting GNRs can be made. Those transistors which are having larger carrier mobility can perform potentially better.

GNRs are considered as a potential candidate because of large MFP of electrons in graphene. Large current densities also exist in graphene. For the VLSI interconnect applications, the metallic nature of CNT and GNR are required. The fabrication process is more complex in deep sub micron technology and CNTs have non planar nature, so we prefer GNRs for interconnect as GNR can be easily maufacturable and patternable using the conventional lithography.

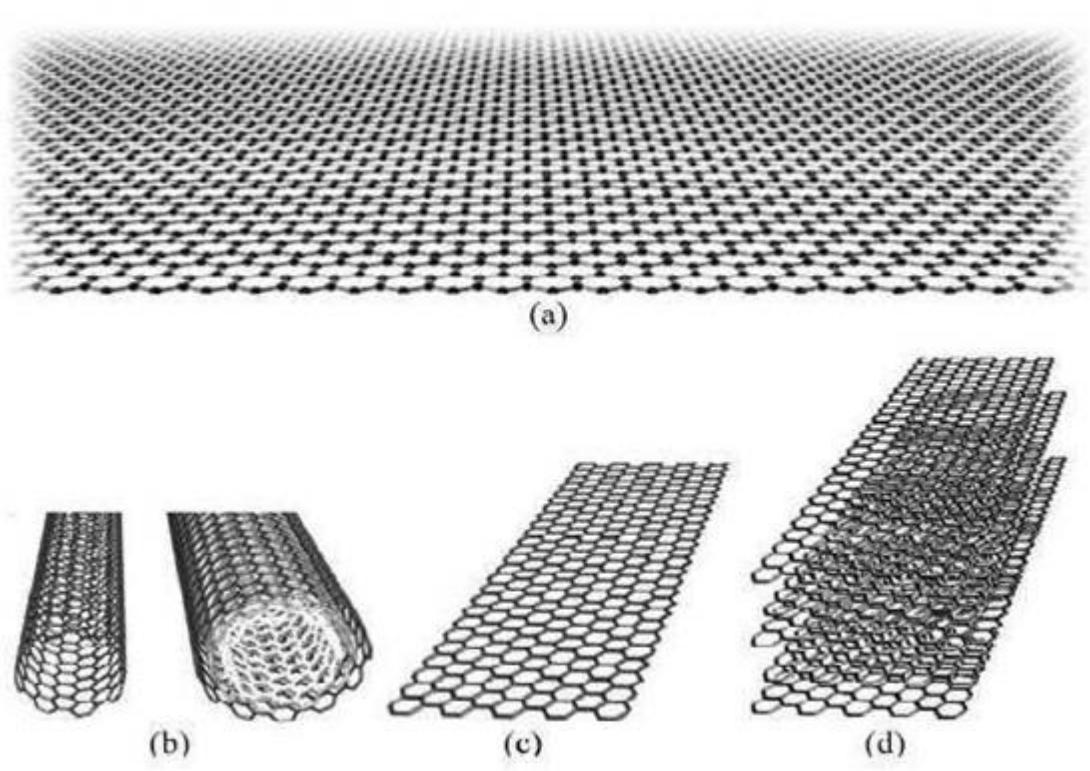

Figure 1.3 Graphene Structures a) Graphene sheet b) CNT c) SLGNR d) MLGNR [7]

The Figure 1.3 shows the geometry of various structures of graphene [7]. Figure (a) shows the geometry of graphene from which different types of interconnects models are made. Figure (b) shows the carbon nano tube which is in the form of hollow cylinder. It can be single walled or multiwalled depending on the type of structure. Figure (c) shows the single layer GNR. However SLGNR is not used because of its low resistance. So, MLGNR is used because of its lower resistance than SLGNR. SLGNR has resistance of the order of kilo ohms. Figure (d) shows the multi layer GNR. In MLGNR, Vander walls forces are present between layers. So the interaction between different layers is weak. So the MLGNR characteristics are almost similar to that of graphene [7]. The total number of Layers in MLGNR depends on the thickness and spacing between each layer.

1.3.1 Classification of GNR Interconnects

There are two types of lithography on the basis of chirality, Arm chair GNRs (ac-GNR) and Zigzag GNRs (zz-GNRs) are the types. The arm chair graphene nano ribbons are classified as metallic and semiconducting depending on the number of hexagonal rings presents across the width of GNRs. The numbers of hexagonal rings are fixed along the length. In arm chair GNRs, if n= 3q-1 or N= 3q+2 then the GNR is metallic in nature and if N= 3q or 3q+1, the GNR is semiconducting in nature where N is the number of hexagonal rings and q is integer.

On the basis of number of layers, the classification of GNR is as single layer GNR (SLGNR) and multilayer GNRs (MLGNR). Monolayer graphene has a large mean free path and large conductivity. MLGNR turns to graphite band have lower conductivity per layer due to intersheet electron hopping. Edge scattering exists in GNR which reduces the mean free path while there is not such issue of scattering in CNT. Due to very high resistance of mono layer graphene, it is essential to use MLGNR. Moreover, the GNR conductance can be increased by doping [8]. Intercalation doping affects the performance of Multilayer GNR. Figure 1.4 shows a single layer GNR interconnect where a sheet of GNR is placed over a dielectric material [8]. $\mathcal{E}_r$ is the permittivity of medium and d is the length of dielectric material.

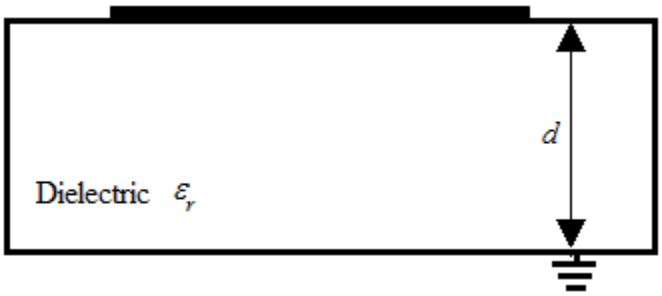

Figure 1.4 Single-layer GNR interconnect [8]

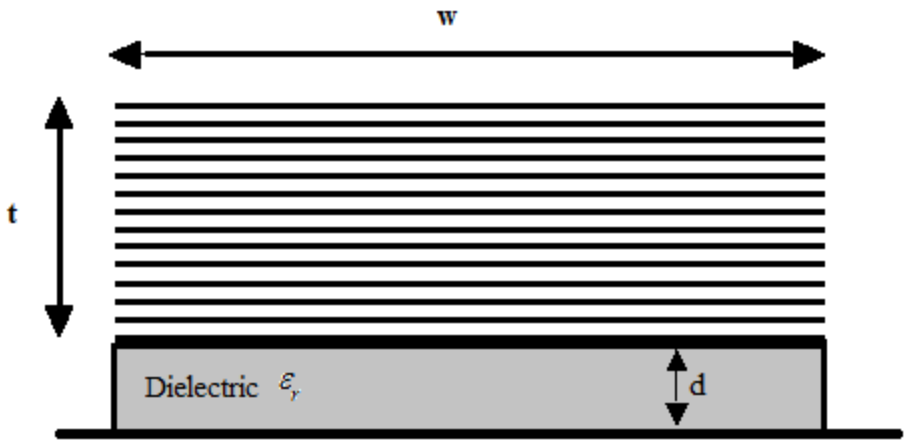

Figure 1.5 Multi-layers GNR interconnects [38]

A MLGNR is placed above the ground by distance d as shown in Figure 1.5. W and t are the width and the thickness respectively. $\mathcal{E}$ is the permittivity of the medium between the ground and the bottom most layer of GNR [8]. The total number of layers is dependent on the *t* and interlayer distance (δ). The parameter δ is assumed to be 0.575 nm and 0.34 nm for doped and neutral MLGNR.

Intercalation doping effects can be come into existence to improve the MLGNR performance. The graphene sheets of high quality have large MFP in the range of 1-5um resulting in

ballistic transport phenomenon. The carrier mobility of GNR is high having value of $3*10^3$ cm^2V^{-1}. And have high current density as compared to copper. SLGNR have high resistivity. So, MLGNR are preferred over SLGNR due to their low resistivity. The in plane conductivity of GNR can be increased upto 30 times by the use of intercalation doping because the mean free path is increased by intercalation doping due to an increase in spacing between adjacent layer. The stacking of layers suggests the GNR as single layer GNR and multilayer GNR. In SLGNR, only one layer is placed at distance d from ground. However SLGNR is not used because of its low resistance. So, MLGNR is used because of its lower resistance than SLGNR. SLGNR has resistance of the order of kilo ohms. In MLGNR, Vander walls forces are present between layers. So the interaction between different layers is weak. So the MLGNR characteristics are almost similar to that of graphene. The total number of Layers in MLGNR depends on the thickness and spacing between each layer.

1.3.2 Single Layer GNR Interconnects

Single layer graphene nano ribbons are the building blocks of multilayer GNR interconnects. The resistance of single layer GNR is very high. So incompatible to use without any modification in design. To understand the various parameters, an equivalent RLC model is used consisting of various inductors, resistors and capacitors.

1.3.3 Equivalent RLC model of Single Layer GNR Interconnects

Single layer RLC model is used to derive the ESC model of the MLGNR, so it is very important to understand the various parameters affecting the performance. Due to the imperfect contact between transistors and interconnect, a resistance is developed between them called as contact resistance having value of 3.2kΩ. When the length of interconnect is greater than the effective mean free path, its scattering resistance is taken into account. There are two type of inductance involved in interconnect modeling, these are kinetic inductance and magnetic inductance. The kinetic inductance represents the kinetic energy of electrons while the magnetic inductance provides the energy stored in magnetic field. There are two types of capacitors involved; these are quantum capacitance and electrostatic capacitance. The quantum capacitance is due to the density of electronic states whereas the electrostatic capacitance is due to the coupling between different layers of GNR. The equivalent inductance decreases as the number of layer increases. All these parameters affects the propagation delay, power dissipation and power delay product of multi layer graphene nano ribbon interconnect.

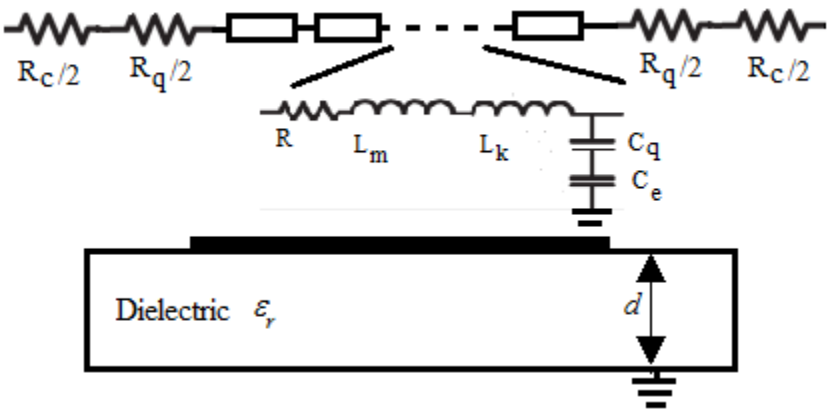

Figure 1.6 Equivalent RLC model of SLGNR interconnects [8]

Figure 1.6 shows the equivalent RLC circuit model of SLGNR interconnects [38].When the length of interconnect is greater than the effective mean free path, its scattering resistance is taken into account. There are two type of inductance involved in interconnect modeling, these are kinetic inductance and magnetic inductance. The kinetic inductance represents the kinetic energy of electrons while the magnetic inductance provides the energy stored in magnetic field. There are two types of capacitors involved; these are quantum capacitance and electrostatic capacitance. The quantum capacitance is due to the density of electronic states whereas the electrostatic capacitance is due to the coupling between different layers of GNR.

1.3.4 Multi-Layer GNR Interconnects

In multilayer graphene nano ribbon interconnects, Vander walls forces are present between layers. So the interaction between different layers is weak. So the multi layer graphene nano ribbon characteristics are almost similar to that of graphene. The total number of Layers in multi layer graphene nano ribbon depends on the thickness and spacing between each layer. Multi layer graphene nano ribbon turns to graphite band have lower conductivity per layer due to intersheet electron hopping. Edge scattering exists in graphene nano ribbon which reduces the mean free path while there is not such issue of scattering in carbon nano tube [9]. Due to very high resistance of mono layer graphene, it is essential to use multi layer graphene nano ribbon. Moreover, the graphene nano ribbon conductance can be increased by doping. The previous research showed that the interlayer distance interactions can be cancelled out by controlling the stacking sequences of the layers where the achieved multi layer graphene nano ribbon can have the same characteristics to that of an isolated single layer graphene sheet.

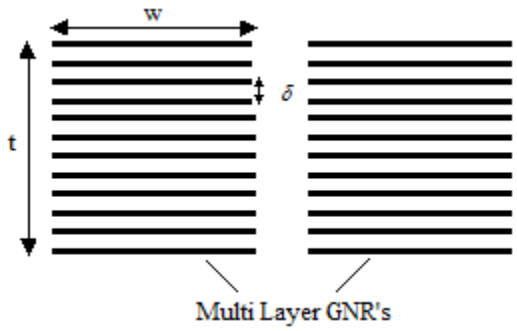

Figure 1.7 Un-doped MLGNR interconnects [8]

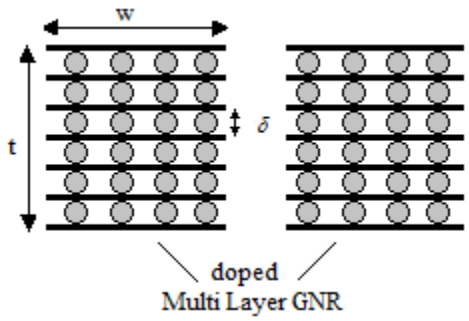

Figure 1.8 MLGNR interconnects with intercalation doping [8]

Figure 1.7 and Figure 1.8 shows the undoped and doped MLGNR interconnect [8]. W and t are the width and the thickness respectively. Ɛ is the permittivity of the medium between the ground and the bottom most layer of GNR. The total number of layers is dependent on the *t* and interlayer distance (δ). The parameter δ is assumed to be 0.575 nm and 0.34 nm for doped and neutral MLGNR. Intercalation doping effects can be come into existence to improve the MLGNR performance. The graphene sheets of high quality have large MFP in the range of 1-5um resulting in ballistic transport phenomenon. The carrier mobility of GNR is high having value of $3*10^3$ cm^2V^{-1} and have high current density as compared to copper.

The process induced parameter variations like dielectric thickness, interconnect width, dielectric constant, mean fee path impacts the performance of multi layer graphene nano ribbon. There are many other parameters which affect the overall delay performance of multi layer graphene nano ribbon [1]. These parameters are interlayer distance, doping concentration and imperfect metal multi layer graphene nano ribbon contact resistance. The stacking of graphene layers forms a bulk graphite. With the increase in the number of layers in multi layer graphene nano ribbon, the interactions between the layers forms a transition from the two dimensional graphene to the bulk graphite. The resistance of multilayer graphene nano ribbon interconnects decreases on increasing the number of layers. So, the mono layer graphene nano ribbon has high resistance than MLGNR interconnect.

1.3.5 Analysis of GNR as a VLSI interconnects

In interconnects, to derive an interconnect loads, CMOS is used. The desired NMOS and PMOS ratio are selected according to the ITRS standards. Parameters are taken from the ITRS 2013. The interconnect wire is broken into the passive components. The optimum number of repeaters are used to decrease the propagation delay of interconnect at the cost of increasing the power dissipation.

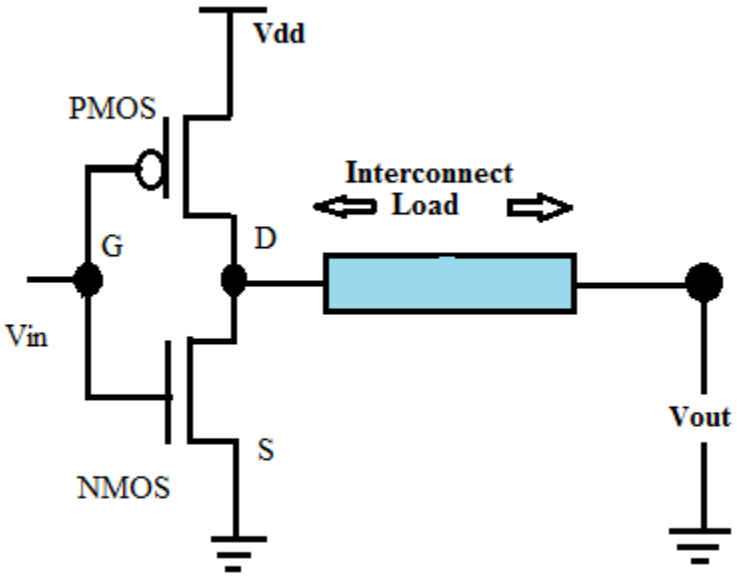

Fig 1.9 CMOS driving an interconnect load

1.3.6 Thesis organization

Thesis consists of six chapters showing the performance of multilayer GNR interconnects in terms of propagation delay and power dissipation at different technology nodes.

Chapter 1 The introduction of interconnects materials is contained in this chapter. Various structures for the VLSI interconnect materials are also discussed in this chapter.

Chapter 2 Literature survey related to the topics is discussed in this chapter. In order to understand the thesis, the first step is to study the information available about related topic.

Chapter 3 Research gaps found in the literature survey are discussed in this chapter. According to these research gaps, the objectives of thesis are selected.

Chapter 4 covers the proposed methodology for objectives. It contains the DIL load and various mathematical equations which are used to analyze the performance of Graphene Nano Ribbons as interconnect material**.** The method to solve the mathematical equation and simulate the MLGNR to obtain propagation delay and power dissipation is studied**.**

Chapter 5 discusses the results based on proposed methodology.

Chapter 6 contains the conclusion and future scope of MLGNR as a interconnect material. According to obtained results, the applicability of MLGNR in interconnects applications and its potential to replace copper as VLSI interconnects is studied.

CHAPTER 2
LITERATURE REVIEW

On the Modeling of Resistance in GNR for Future Interconnect Applications [3]

T. Ragheb, and Y. Massoud

In this paper, the MLGNR structure and the effect of stacking layer model is used to perform comparison of MLGNR CNR and copper interconnect. The result obtained clearly shows the replacement of copper and carbon nano tubes interconnects at width less than 15nm. So for high packaging requirements, GNR can replace both copper as well as carbon nano tubes.

Time and Frequency Domain Analysis of MLGNR Interconnects [4]

V.Kumar, Manoj Kumar, and B.K Kaushik

This paper analyzes the performance comparison of copper and multi layer graphene nano ribbon interconnects with different conditions of edge roughness. A narrow width multi layer graphene nano ribbon exhibits rough edges due to which mean free path is reduced. So the resistance increases. For multi layer graphene nano ribbon the doping is inevitable because the conductivity of neutral multi layer GNR is lower than even copper. This paper compares and analyzes the delay, power dissipation and bandwidth performance of copper and MLGNR using an equivalent single conductor model.

Analytical Time-Domain Models for Performance Optimization of Multilayer GNR Interconnects [5]

Atul K. Nishad, and Rohit Sharma

In this paper, the analytical time domain models for top contact and side contact MLGNR interconnects are proposed. The proposed models analyze the transient behaviour of multi layer graphene nano ribbons. The excellent accuracy has been achieved by the transient behaviour of MLGNR. Limiting factors are analyzed based on the analysis and are considered for the design of optimum top contact multi layer graphene nano ribbons that is far better than the performance of copper interconnects. The performance of top contact multi layer GNR is also compared with optical interconnects.

Resistivity of Graphene Nanoribbon Interconnects [6]

Raghunath Murali, Kevin Brenner, Yinxiao Yang, Thomas Beck, and James D. Meindl

This paper represents the first experimental results to replace copper with narrow graphene nano ribbons as VLSI interconnects. Graphene nano ribbons were manufactured and

compared with copper in terms of 3-D resistivity. The average GNR resistivity was calculated higher than that of Cu resistivity with the feature size between 18 nm and 52 nm. Resistivity of individual GNR was calculated from the MLGNR and it was found that the best GNR with appropriate width have the resistivity similar to that of copper interconnect for similar dimensions.

GNR Interconnects: A Genuine contender or a delusive dream [7]

C. Xu, H. Li, and K. Banerjee

In this paper, the conductance and delay analysis of GNR are modeled and the resistance, inductance and capacitance values are derived. Electrostatic inductances and quantum capacitances are the components of distributes capacitances. Similarly the kinetic inductance and magnetic inductances are the components of distributed inductance. At different technology nodes, the GNR and other interconnect materials are compared. Beyond 22nm, single walled CNTs are the best but all the graphene nano ribbons are poor than copper for local and global interconnect. Intercalation doping effect is studied and is concluded that by increasing the intercalation doping, the conductivity increases simultaneously. It is concluded that MLGNR have the properties comparable to copper.

Performance Improvement in SC-MLGNRs Interconnects Using Interlayer Dielectric [8]

Atul Kumar Nishad, and Rohit verma

In this paper, the impact of dielectric layer insertion on propagation delay, power dissipation and bandwidth of GNR is studied. The results show that by inserting dielectric layer, the Performance of MLGNR is increased. The reduction in both delay and power dissipation is observed along with improvement in bandwidth.

Number of Conducting Channels for Armchair and Zigzag GNR Interconnects [9]

Antonio Maffucci, and Giovanni Miano

In this paper the kinetic inductance and the quantum capacitances are expressed in terms of number of conducting channels. The exact variation of number of conducting channels along with the width is studied and it is concluded that the number of conducting channels derived in the theory is much over estimated when compared with the actual results. This is analyzed by taking the exact distribution of the energy spectrum and the velocity of the conduction electrons.

Comparable study on MLGNR interconnects [10]

Wen-Sheng Zhao, and Wen-Yan Yin

In this paper, the transmission analysis and performance of multilayer graphene nano ribbon interconnects is studied. The derivation of analytical equations for characterizing the multilayer graphene nano ribbon interconnects are studied which is based on the equivalent semiconductor model. The further analysis of electrical performance based on ITRS 2010 is compared with copper and carbon nano tube interconnects. The effect of crosstalk on the multilayer graphene nano ribbon interconnects is analyzed. The induced time delay and noise due to the crosstalk is analyzed and characterized.

Signal Integrity analysis of Graphene Nano-Ribbon (GNR) Interconnects [11]

Wen-Sheng Zhao, and Wen-Yan Yin

Graphene nano-ribbons (GNR) have been proposed as to build the 3-D Integrated circuits due to the better performance over conventional metallic materials. Signal integrity analysis of single layer graphene nano ribbon and multi layer graphene nano ribbon interconnects are carried out in this paper based on the equivalent circuit models with the crosstalk effects. It is analyzed that larger width and longer length of SLGNR interconnect results in the high crosstalk voltage but it cannot be greater than the threshold voltage.

Modeling, Analysis and design of Graphene Nano Ribbon Interconnects [12]

C.Xu, H.Li, and K.Banerjee

In this paper, a study on conductance and RLC model is done. The landauer formula is used to obtain the conductance model of GNR. The GNR conductance is compared with other VLSI interconnect materials i.e. copper, CNT and W. Intercalation doping is also used. Edge scattering phenomenon is the main problem of GNR which reduces the effective mean free path. Conductivity per layer is affected by inter- sheet hopping. Intercalation doping increases the in plane conductivity of GNR by 100 times. Intercalation doping is done by adding 1 dopant layer between each graphene layer. Due to this, the carrier density increases due to the charge transfer causing the increase in mean free path. The delay ratio of graphene nano ribbon is also compared with copper which concludes that the intercalation doping and specular edges ($p > 0.5$) are needed to make MLGNR comparable to CNT and copper. . Edge scattering phenomenon is the main problem of GNR which reduces the effective mean free path.

Carbon Nano materials for next generation interconnects and Passives [13]

H.Li, C. Xu, N. Srivastava, and K. Banerjee

In this paper, different models of CNT and GNR are studied. Single walled CNTs**,** double walled CNTs and multiwalled CNTs are compared with copper. The result showed that all of these are potential candidate in comparison to copper as VLSI interconnects. To compete GNR with CNT and copper, the intercalation doping is used because the intercalation doping increases the conductivity of undoped GNR. CNTs are better for the circuits operating at very high frequencies because CNTs have very high kinetic inductance.

Conductance modeling for Graphene Nano Ribbon interconnects [14]

A. Naeemi, and J. D. Meindl

In this paper, the conductance model of GNR is obtained having various types of scattering phenomenon like Fermi level, width, chirality. It is concluded that below 8nm, GNR offers less resistance in comparison to copper. So, metallic GNR is better than copper at 8nm or lower level at the aspect ratio of unity. For GNR with width greater than 100nm, increase in Fermi level increases the conductance but it is not for the smaller width GNR. In this model, contact resistance of GNR is not included because of less data available.

Compact Physics based circuit models for GNR interconnect [18]

A. Naeemi, and J. Meindl

Edge roughness effect due to the manufacturing problem is discussed in this paper. The resistance is compared and the edge roughness impact on the resistivity of GNR is compared. It is found that there is a need to manufacture a GNR having small width and smooth edges. Resistivity of GNR is affected by edge roughness. Due to this propagation delay increases. So good fabrication techniques are needed to replace the copper interconnect. New patterning methods are needed to produce the smooth edges GNR so as to get the low resistance of graphene nano ribbon.

Performance and energy-per-bit modeling of multilayer GNR conductors [20]

V. Kumar, S. Rakheja, and A. Naeemi

The effective resistance of MLGNR interconnect is calculated by deriving the physical models. In this paper, the finite resistive coupling impact between the top layers of MLGNR interconnects is considered. It is not necessary that the overall resistance of multilayer GNR will decrease on increasing the parallel layers of MLGNR interconnect. To get the minimum propagation delay and minimum power delay product, the optimum numbers of layers are

introduced. The effective resistance of multi layer graphene nano ribbon interconnect is analyzed by the mathematical model. The number of layers and edge scattering affects the effective resistance of multi layer GNR interconnect. The delay and energy delay product of MLGNR interconnect are optimized and compared with the copper interconnect. The performance parameters of both the MLGNR and copper interconnect are compared.

Comparison of Propagation Delay in Single- and Multi-layer GNR Interconnects [22]

Manoj Kumar, Majumder, and Narasimha Reddy

In this paper, the effect of propagation delay is studied using an equivalent RLC model for multi layer graphene nano ribbon interconnects. The width and scattering effects of graphene nano ribbon are also considered. The comparison of propagation delay in single layer GNR and multi layer GNR interconnect is done. To get the minimum delay, the optimum value of number of layers is calculated.

Performance Benchmarking for Graphene Nano ribbon, Carbon Nanotube and Cu interconnects [26]

Azad Naeemi and James D. Meindl

The equivalent circuit models for armchair and zigzag graphene nano ribbons are analyzed in this paper. The conductance of armchair and zigzag GNR have been benchmarked against the copper and carbon nano tubes interconnects. The thick graphene nano ribbons having smooth edges can potentially have smaller resistances in comparison to the copper interconnects with unity aspect ratios for width lesser than 8nm. . It is found that there is a need to manufacture a GNR having small width and smooth edges.

Optimized Delay and Power Performances in MLGNR Interconnects [29]

Narasimha Reedy, Manoj Kumar and B.K Kaushik

Multilayer graphene nano ribbon interconnects are considered as a potential candidate for interconnect material in nano scale and deep submicron technology. An equivalent RLC model for MLGNR interconnects is presented in this research paper which is primarily based on the geometry. Propagation delay, power dissipation and power delay product is analyzed in this paper for different technology nodes. It is found that there is a need to manufacture a GNR having small width and smooth edges. Resistivity of GNR is affected by edge roughness. Due to this propagation delay increases. The delay and energy delay product of MLGNR interconnect are optimized and compared with the copper interconnect.

Signal Transmission Analysis of MLGNR Interconnects [32]

Wen-Yan Yin, Wen-Sheng Zhao, and Jun Hu

In this paper, the signal transmissions characteristics of multi layer graphene nano ribbon interconnect are analyzed using an equivalent single conductor model. Both inductive and capacitive coupling between the layers of graphene nano ribbon are realised. The output voltage waveforms are observed for 14nm and 22nm technology node. The effect of fermi level of multi layer graphene nano ribbon on the time delay of transmitted rectangular pulse are compared and examined with the copper interconnects. The output voltages waveforms are predicted for the different technology nodes.

Review of Multi-Layer GNRs for on-chip Interconnect Applications [33]

Vachan Kumar, Shaloo Rakheja, and Azad Naeemi

This paper presents the analytical models for transmission of signals in MLGNR interconnects. The current is distributed between the layers of GNR using the analytical models. The multi conductor transmission line models are used to show the current distribution between the layers of GNR. The optimum number of layers of GNR are calculated to reduce the propagation delay and power delay product of interconnect. Energy delay product is reduced by optimizing the number of layers.

The multi conductor transmission line model and the equivalent RC models for multilayer GNR are analyzed to predict the performance of MLGNR in digital circuits. The computation of frequency response, propagation delay and energy consumed by MLGNR interconnect by the analytical models is studied. The performance parameters are compared with the copper interconnects.

Circuit Modeling of MLGNR interconnects [34]

Yuan Fang, Wen-Sheng Zhao, and Wen-Yan Yin

Circuit modeling of SLGNR and MLGNR is done in this paper. The capacitive and inductive coupling impact is calculated. The delay ratio of MLGNR with copper is considered. The contact resistance affects the delay of MLGNR interconnects and is concluded that 3% variation occurs when contact resistance is included.

Stability Analysis in GNR interconnects [35]

S. H. Nasiri, Md. K. M. Farshi, and R. Faez

The analytical model for the calculation of number of layers and number of channels of GNR interconnect is represented in this paper. The typical equation of number of channels of

MLGNR is solved by looping method and simplified formula is obtained. It is found that the result accuracy is 1% of exact formula. Width, Fermi and temperature affect the number of channels. Different mathematical equations are developed at zero Fermi level.

Comparative Study on Multilayer Graphene nanoribbon (MLGNR) Interconnects [36]

Wen-Sheng Zhao, Wen-Yan Yin

They investigated the transmission performance of MLGNR interconnects with side and top contacts theoretically based on their ESC model. They found that the number of conducting channels of a metallic MLGNR interconnect is the linear function of its width and Fermi energy. They also developed the Equivalent inductance and capacitance equations for the ESC model.

It was demonstrated that the side contacts in MLGNR interconnects can achieve smaller resistance in comparison with that of top one for short interconnect length.

They proved that MLGNR interconnects can provide better performance than Cu wires in particular at intermediate level. According to them the edge roughness and Fermi energy are two important factors affecting the performance of MLGNR interconnect.

Performance Analysis of MLGNR in Current Mode Signalling Interconnect System [42]

Yash Agrawal, Rajeevan Chandel, and M.G Kumar

Graphene nano ribbon is considered as the potential material for on-chip interconnects material.

Current mode signalling is better in comparison to the conventional mode signalling system. Current mode signalling system needs more investigation. This paper analyzes the MLGNR using CMS. Band width, delay and power dissipation are analyzed for current mode signalling system. The performance of current mode signalling MLGNR is compared with current mode signalling copper interconnects. It is observed that with increase in the length of interconnect, propagation delay increases but propagation delay and power dissipation decreases. The impact of signal transitions period variations is also observed. The signal transitions affect the performance of system.

Performance Analysis of Multilayer graphene nanoribbon (MLGNR) interconnects [43]

Mayank Kumar Rai, A.K Chatterjee, Sankar Sarkar, and B.K Kaushik

The impact of interlayer resistance and contact resistance on performance is addressed in terms of propagation delay, power dissipation and power delay product for the multi layer graphene nano ribbon interconnects. The impact of fermi energy on the performance of

MLGNR is also discussed. The results are compared with copper at 22nm technology node. The impact of interlayer resistance on equivalent resistance of multi layer graphene nano ribbon is also analyzed. In this analysis the inductive and capacitive coupling are also included. It is observed that multi layer graphene nano ribbon with interlayer resistance gives better performance in terms of propagation delay, power dissipation and power delay product in comparison to the copper interconnect.

CHAPTER 3
RESEARCH GAPS

The literature work shows that the copper resistivity increases drastically as technology scales down below 45nm. The performance of copper interconnect degrades when feature size becomes close to mean free path of copper (45nm). So it is essential to replace copper interconnects in deep sub micron region. GNR interconnects are the potential candidate to replace copper for future interconnect applications. The impact of fermi energy on propagation delay and power dissipation is not analyzed in literature. The impact on propagation delay and power dissipation will be considered at different technology nodes and length. Further, the impact of interlayer distance is need to evaluate.

3.1 OBJECTIVES

1. To develop the equivalent impedance model for MLGNR interconnects.
2. To analyze the impact of Fermi energy on the impedance parameters of MLGNR for different technology nodes.
3. To analyze the impact of Fermi Energy on the performance in terms of propagation delay and power dissipation of MLGNR Interconnects.
4. To analyze the impact of interlayer distance of MLGNR and estimate the performance for propagation delay, power dissipation and power delay product (PDP).
5. To compare the results obtained from above objectives at different technology nodes for variable interconnect length.

CHAPTER 4

PROPOSED METHODOLOGY

The multi-layer GNR interconnect is modeled into equivalent single conductor model. The RLC components of the associated layer are calculated using mathematical equations. The equations are solved in MATLAB and simulated in T-SPICE.

The layers of GNR are placed at distance d from ground. The permittivity of medium is $\mathcal{E}_r$ and thickness of GNR layers is t. W is the width of interconnect line. Figure 4.1 shows the MLGNR interconnect on a substrate.

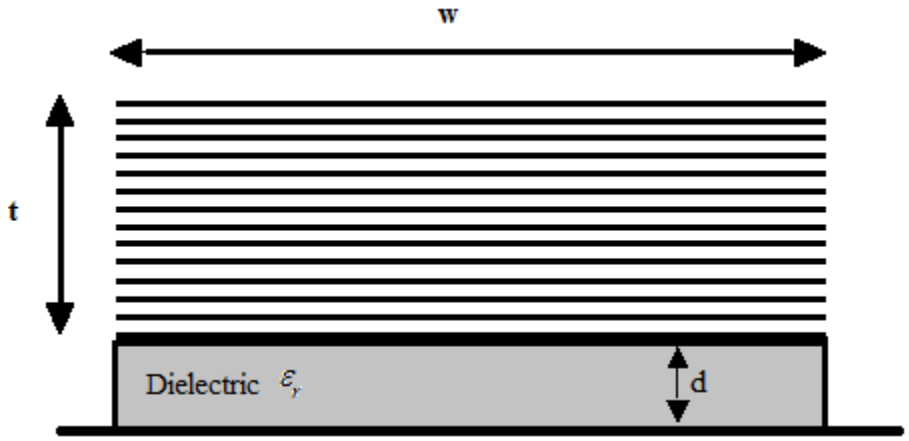

Figure 4.1 Multilayer GNR interconnect on a substrate

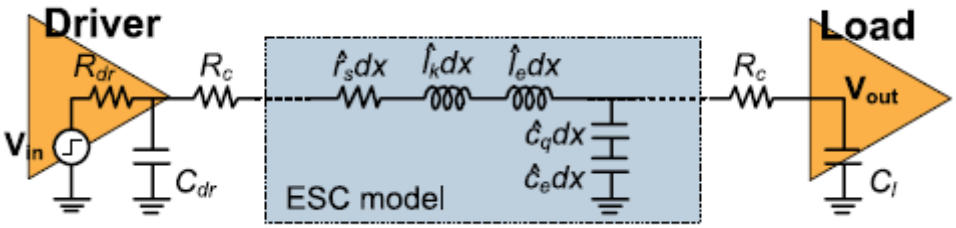

Figure 4.2 Equivalent Single Conductor Model

Figure 4.2 shows the ESC model of Multilayer GNR interconnects. The number of layers are stacked one above the other, where w is the width, t is the thickness, d is the height of MLGNR above the ground plane, Ɛ is the dielectric constant and delta is the distance between the layers. $^{\delta}$ is assumed to be 0.34nm. as the layers in multilayer GNR can be viewed as the stacked single layer GNR and therefore the total number of layers is determined by n. the intervals facing between the adjacent layers is d=0.34 nm which is the vanderswall gap. The total number of layers is determined by $n = 1 + \text{int}(\frac{H}{\delta})$ where int (.) means to consider only integer part.

The number of channels per layer for a given width of metallic ac-GNR is given by

$N_{ch} = \alpha W E_F$, $E_F \geq 0.1$eV & W>10nm

Where the interconnect width w is in nanometer, Fermi energy is in electron volt and α= 1.2 $eV^{-1}nm^{-1}$.

Table 4.1 Number of conducting channels per layer as a function of Fermi energy for metallic armchair GNR

Fermi Energy E_F	No. of conducting channels (Nch) at W= 15nm	No. of conducting channels (Nch) at W= 22.5nm	No. of conducting channels (Nch) at W= 24nm	No. of conducting channels (Nch) at W= 36nm
0.1	1.8	2.7	2.88	4.32
0.2	3.6	5.4	5.76	8.64
0.3	5.4	8.1	8.64	12.96
0.4	7.2	10.8	11.52	17.28
0.5	9	13.5	14.4	21.6
0.6	10.8	16.2	17.2	15.92

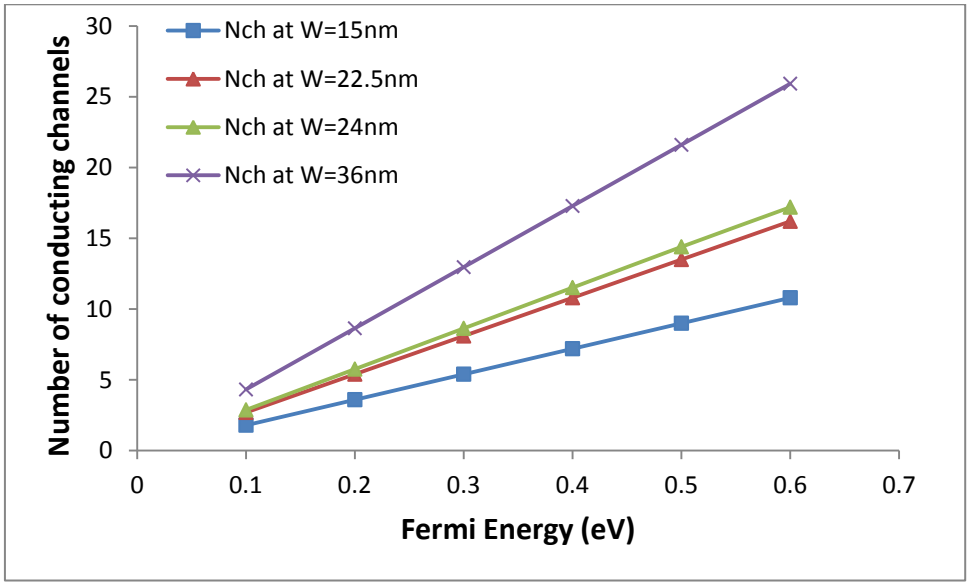

Figure 4.3 Number of conducting channels per layer as a function of Fermi energy for metallic armchair GNR

The number of conducting channels increases with the increase in Fermi energy. Figure 4.3 shows the plot between the number of conducting channels per layer as a function of Fermi energy. Figure 4.4 shows the plot between number of conducting channels per layer as a

function of width. As interconnect width increases, the number of conducting channels starts increases.

Table 4.2 Number of conducting channels per layer as a function of Width for metallic armchair GNR

Width (nm)	No. of conducting channels (Nch) at E_F = 0.2eV	No. of conducting channels (Nch) at E_F = 0.4eV	No. of conducting channels (Nch) at E_F = 0.6eV
10	2.4	4.8	7.2
20	4.8	9.6	14.4
30	7.2	14.4	21.6
40	9.6	19.2	28.8
50	12	24	36
60	14.4	28.8	43.2
70	16.8	33.6	50.4
80	19.2	38.4	57.6
90	21.6	43.2	64.8
100	24	48	72

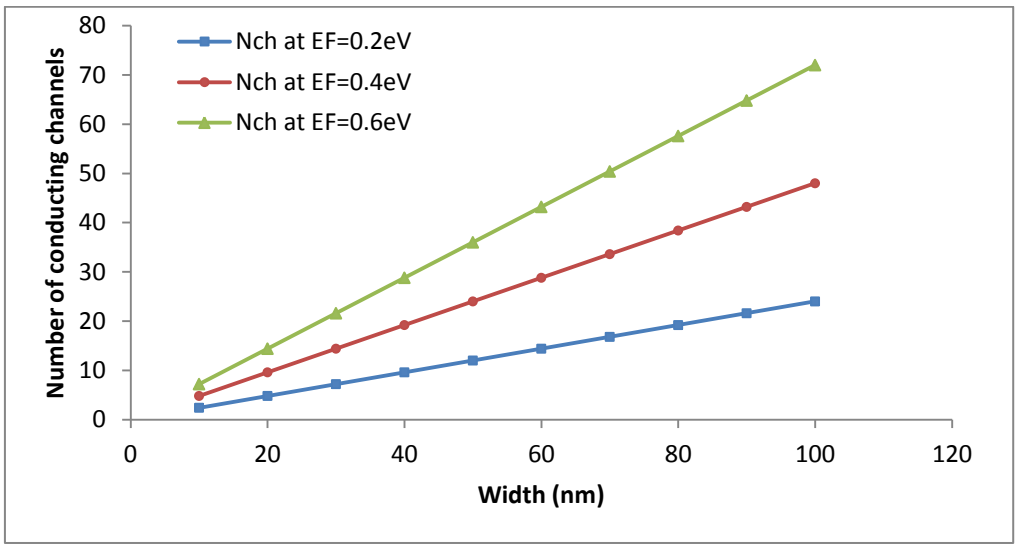

Figure 4.4 Number of conducting channels per layer as a function of Width for metallic armchair GNR

A) Equivalent Resistance

When the length of interconnect is greater than the effective mean free path, its scattering resistance is taken into account. The total scattering resistance is given by

$$R_s = \frac{12.9}{nN_{ch}} k\Omega \quad (4.1)$$

The quantum contact resistance $R_q = \frac{12.9}{N_{ch}} k\Omega$ of SLGNR is determined by the number of conducting channels N_{ch}, which is a function of width and Fermi energy.

The contact resistance is given by

$$R_c = \frac{R_q}{2n} = \frac{6.45}{nN_{ch}} k\Omega \quad (4.2)$$

The net equivalent resistance is given by

$$R_{eq} = 2R_c + R_s L \quad (4.3)$$

B) Equivalent Inductance

There are two type of inductance involved in interconnect modeling, these are kinetic inductance and magnetic inductance. The kinetic inductance represents the kinetic energy of electrons while the magnetic inductance provides the energy stored in magnetic field.

The magnetic inductance is given by

$$L_e = \frac{\mu d}{W} nH / \mu m \quad (4.4)$$

Where μ= Permeability of medium= $12.5*10^{-7}$ H/m

d= interlayer distance

w= width of interconnect material

The Kinetic inductance is given by

$$L_K = \frac{8}{n\alpha W E_F} = \frac{8}{nN_{ch}} nH / \mu m \quad (4.5)$$

The equivalent kinetic inductance decreases as the number of layer increases as is shown in the Figure 4.5.

The net equivalent inductance is given by

$$L_{eq} = (L_K + L_e) * L \text{ nH} \quad (4.6)$$

The equivalent inductance obtained by using the expression (4.5) is plotted in Figure 4.5. The plot between the ESC Kinetic inductance as a function of layer number is shown in the Figure 4.5.

Table 4.3 Equivalent Inductance in the ESC model of MLGNR interconnect as a function of layer number

Layer Number N	ESC Kinetic Inductance at E_F = 0.2eV	ESC Kinetic Inductance at E_F = 0.4eV	ESC Kinetic Inductance at E_F = 0.6eV
10	0.222	0.111	0.074
20	0.111	0.055	0.037
30	0.074	0.037	0.024
40	0.055	0.027	0.018
50	0.044	0.022	0.014
60	0.037	0.018	0.012
70	0.031	0.015	0.01
80	0.027	0.013	0.009
90	0.024	0.012	0.008
100	0.022	0.011	0.007

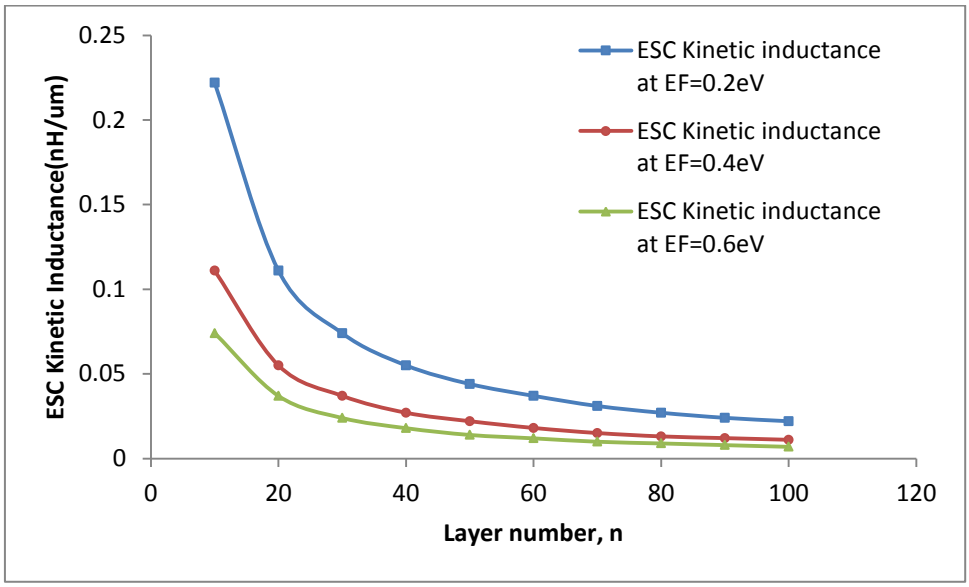

Figure 4.5 Equivalent Inductance in the ESC model of MLGNR as a function of layer number

C) Equivalent capacitance

There are two types of capacitors involved; these are quantum capacitance and electrostatic capacitance. The quantum capacitance is due to the density of electronic states whereas the electrostatic capacitance is due to the coupling between different layers of GNR.

The electrostatic capacitance is given by

$$C_e = \frac{\varepsilon W}{d} \text{ aF/um} \quad (4.7)$$

Where Ɛ = Permittivity of free space = $8.854*10^{-12}$ F/m

The quantum capacitance is given by

$$C_q = 100\alpha W E_F \left[1 + \sqrt{1 + \frac{1}{\alpha W E_F}}\right] \quad (4.8)$$

The equivalent capacitance of MLGNR interconnect is nearly a constant as shown in the Figure 4.6

Net equivalent capacitance is

$$C_{eq} = \frac{1}{\frac{1}{C_q} + \frac{1}{C_e}} * L \text{ fF} \quad (4.9)$$

Table 4.4 Equivalent Capacitance in the ESC model of MLGNR interconnect as a function of layer number

Layer Number N	ESC Quantum Capacitance at E_F = 0.2eV	ESC Quantum Capacitance at E_F = 0.4eV	ESC Quantum Capacitance at E_F = 0.6eV
0	0.72	1.44	2.16
10	1.3	1.75	2.5
20	1.3	1.75	2.5
30	1.3	1.75	2.5
40	1.3	1.75	2.5
50	1.3	1.75	2.5
60	1.3	1.75	2.5
70	1.3	1.75	2.5
80	1.3	1.75	2.5
90	1.3	1.75	2.5
100	1.3	1.75	2.5

The equivalent inductance obtained by using the expression (4.8) is plotted in Figure 4.6. The plot between the ESC Quantum capacitance as a function of layer number is shown in the Figure 4.6. The coupling capacitance between the adjacent layers of MLGNR is same.

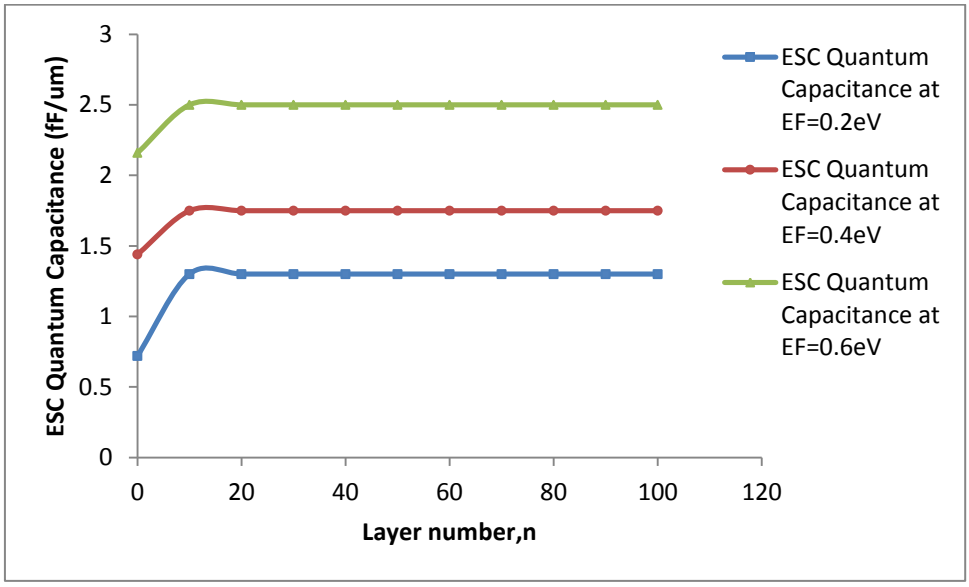

Figure 4.6 Equivalent Capacitance in the ESC model of MLGNR interconnect as a function of layer number

Conductance of MLGNR interconnects

The conductance of GNRs is derived using the linear response Landauer formula which is given by

$$G_n = \frac{2q^2}{h}\int T_n(E)\left(\frac{\partial f_0}{\partial E}\right)dE \tag{4.10}$$

Fermi Dirac function is given by

$$f_0(E) = \left[1+\exp\left(\frac{E-E_f}{kT}\right)\right]^{-1} \tag{4.11}$$

Where q is the elementary charge, $T_n(E)$ is the transmission coefficient and h is planks constant. Total conductance of single layer GNR is given by

$$T_n(E) = \left[1+L\left(\frac{1}{l_D\cos\theta}+\frac{1}{W\cot\theta}\right)\right]^{-1} \tag{4.12}$$

$$\cot\theta = \sqrt{\frac{E^2-E_n{}^2}{E_n}}$$

$\frac{W\cot\theta}{L}$ is the transmission coefficient due to edge scattering when complete diffusive edge is assumed. W cotθ is the distance that electrons/holes travel before hitting the edge.

$\frac{l_D \cos\theta}{L}$ is the transmission coefficient due to defects and phonons scattering. $l_D \cos\theta$ is the average distance that an electron travels along the GNR longitudinal direction before collision.

Edge scattering and scattering by phonons determines the transmission coefficient of MLGNR.

Hence if complete diffusive edge is assumed then transmission coefficient is

$$T_n(E) = \left[L\left(\frac{1}{l_D \cos\theta} + \frac{1}{W \cot\theta} \right) \right]^{-1} \tag{4.13}$$

For narrow ribbons i.e. for W<50nm in the metallic GNR and W<30nm in semiconductor GNRs

Assuming l_D = 1um and E_F = 0.2eV. l_D >> l_n except for n=0 in metallic GNRs for which there is no edge scattering.

For narrow metallic GNR, the conductance is given by

$$G_m = \frac{2e^2}{h} \frac{1}{1+\frac{L}{l_D}} + \frac{2e^2}{h} \sum_{n\neq 0} \frac{1}{1+\frac{L}{l_n}} \tag{4.14}$$

For lengths longer than mean free path, the conductance is given by

$$G_m = \frac{2e^2}{h} \frac{l_D}{l} + \frac{2e^2}{h} \frac{W}{L} \sum_{n\neq 0} \left(\frac{E_F / \Delta E}{n}\right)^2 - 1 \tag{4.15}$$

So, conductance of long narrow metallic GNR is written as

$$G_m = \frac{2e^2}{h} \frac{l_D}{l} + 1.5 \frac{2e^2}{h} \frac{W^{2.5}}{L} \left(\frac{2E_F}{hV_F} \right)^{1.5} \tag{4.16}$$

This term is a strong function of width and fermi energy because it determines the mean free path of the channels other than the one corresponding to n=0. However for narrow metallic GNRs (< 20nm) with diffusive edge scattering, there is no effect of fermi energy on conductance because of shorter mean free path of additional conducting modes. On the basis of physical models, the conductance of graphene nano ribbon interconnects can be calculated as a function of fermi energy, width and chirality. Wide semiconductor and metallic GNRs (> 100nm) have similar conductances Narrow semiconductor GNRs have high resistances. GNRs become insulator at below 5nm widths.

CHAPTER 5
RESULTS

By using the Equivalent single conductor (ESC) model of interconnects, Propagation delay and power dissipation is compared by varying the interlayer distance at 16nm and 22nm technology nodes using the TANNER EDA Tool. For a doped MLGNR, it can be observed that by increasing the interlayer distance up to 0.5nm, the propagation delay is going to decrease for different interconnect lengths of 200,400,600,800 and 1000 μms respectively, but when interlayer distance increases further after 0.5nm, the propagation delay is going to increase for different interconnect lengths. It is also observed that the propagation delay also increases with the interconnect lengths. The propagation delay primarily depends on the resistive and capacitive parasitic. Increasing the interlayer distance reduces the number of layers in MLGNR which increases the resistive parasitic and reduces the capacitive parasitic. From the above discussion, we can also say that the MLGNR can be a potential candidate for the future VLSI interconnects.

Table 5.1 shows the propagation delay at different interlayer distances for variable interconnect lengths at 16nm technology node.

Table 5.1 Propagation delay of MLGNR at different interlayer distances w.r.t Interconnect lengths at 16nm technology node

Length (um)	d=0.34 (nm)	d=0.4 (nm)	d=0.5 (nm)	d=0.55 (nm)	d=0.6 (nm)	d=0.7 (nm)	d=0.8 (nm)	d=0.9 (nm)	d=1 (nm)
100	0.053	0.052	.0518	0.05199	0.0523	0.0528	0.0537	0.0554	0.0565
200	0.115	0.113	0.112	0.1131	0.1141	0.1154	0.1173	0.1209	0.1239
300	0.203	0.199	0.195	0.2011	0.2032	0.2053	0.208	0.2144	0.2192
400	0.316	0.311	0.305	0.3154	0.3188	0.322	0.3253	0.3352	0.3423
500	0.454	0.448	0.4046	0.4557	0.4607	0.465	0.4689	0.4829	0.492
600	0.618	0.609	0.6002	0.6217	0.6287	0.6342	0.6387	0.6573	0.6694
700	0.807	0.795	0.7846	0.8133	0.8225	0.8293	0.8339	0.8583	0.8732
800	1.02	1.005	0.993	1.03	1.0422	1.0505	1.0559	1.085	1.103
900	1.25	1.23	1.226	1.2728	1.2873	1.2968	1.3031	1.339	1.361
1000	1.52	1.503	1.483	1.5404	1.5582	1.5699	1.5759	1.625	1.645

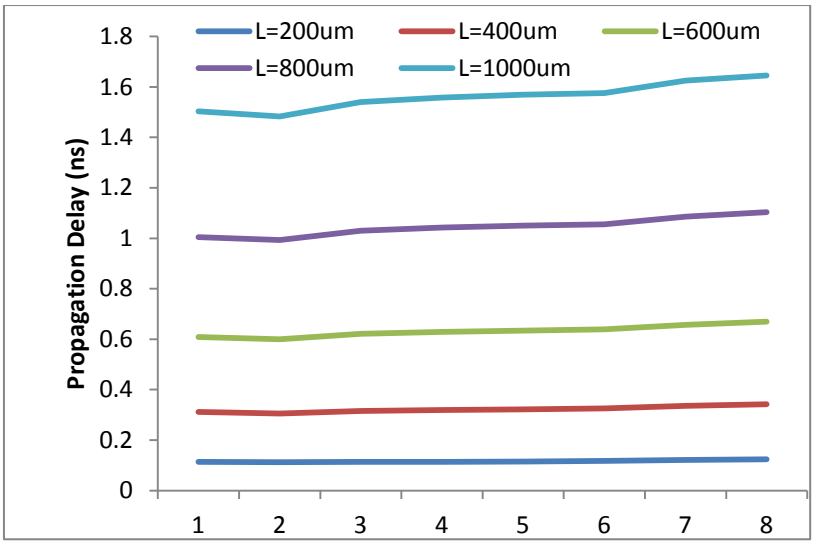

Figure 5.1 Dip showing the optimum interlayer distance of approx. 0.5nm to get the optimum propagation delay of MLGNR at 16nm technology node

The propagation delay at different interlayer distances for variable interconnect lengths at 16nm technology node is shown in Figure 5.1. It can be seen clearly that the dip is shown at the interlayer distance of 0.5nm. At this interlayer distance, an optimum value of propagation delay is estimated for different interconnect lengths.

Table 5.2 Power Delay Product of MLGNR at different interlayer distances w.r.t Interconnect lengths at 16nm technology node.

Length (um)	d=0.34 (nm)	d=0.4 (nm)	d=0.5 (nm)	d=0.55 (nm)	d=0.6 (nm)	d=0.7 (nm)	d=0.8 (nm)	d=0.9 (nm)	d=1 (nm)
100	0.2813	0.2762	0.2707	0.2757	0.2776	0.2799	0.2852	0.2941	0.2999
200	0.5713	0.5529	0.5455	0.6021	0.6164	0.6224	0.6256	0.6344	0.6606
300	1.175	1.067	1.0459	1.117	1.1753	1.1869	1.2025	1.2406	1.2691
400	1.841	1.81	1.7744	1.8365	1.8551	1.8753	1.8958	1.9521	1.9952
500	2.778	2.7408	2.4736	2.7866	2.8199	2.8469	2.8706	2.9589	3.0163
600	3.818	3.7599	3.7028	3.84	3.884	3.9186	3.9474	4.0669	4.1431
700	5.011	4.9584	4.8899	5.0763	5.1351	5.1795	5.2091	5.3684	5.4659
800	6.442	6.3385	6.2606	6.504	6.5843	6.6397	6.6681	6.875	6.994
900	7.995	7.856	7.8207	8.1338	8.2393	8.2956	8.344	8.6571	8.7443
1000	9.857	9.7349	9.594	9.99	10.115	10.195	10.236	10.583	10.7298

Table 5.2 shows the Power Delay Product of MLGNR estimated at different interlayer distances for variable interconnect lengths at 16nm technology node. Figure 5.2 shows the

dip at the interlayer distance of 0.5nm. An optimum PDP is estimated at this interlayer distance. For a doped MLGNR, an optimum interlayer distance of around 0.5nm is needed to get the better performance of MLGNR.

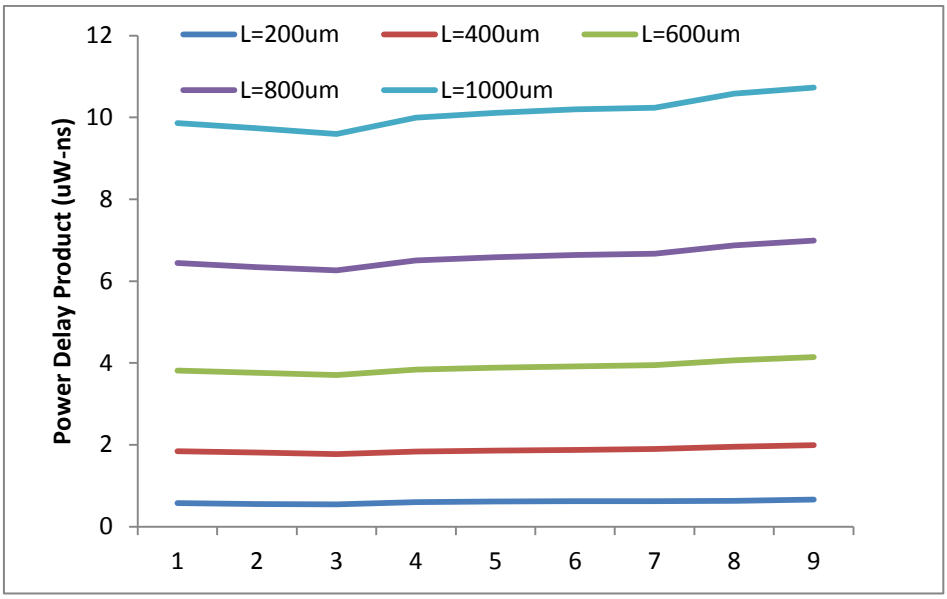

Figure 5.2 Dip showing the optimum interlayer distance of approx. 0.5nm to get the optimum Power Delay Product of MLGNR at 16nm technology node

Table 5.3 Propagation delay of MLGNR at different interlayer distances w.r.t Interconnect lengths at 22nm technology node

Length (um)	d=0.34 (nm)	d=0.4 (nm)	d=0.5 (nm)	d=0.55 (nm)	d=0.6 (nm)	d=0.7 (nm)	d=0.8 (nm)	d=0.9 (nm)	d=1 (nm)
200	0.0909	0.0848	0.0782	0.0791	0.0796	0.0810	0.0824	0.0832	0.0841
400	0.1912	0.1801	0.1681	0.1731	0.1766	0.1841	0.1910	0.1964	0.2009
600	0.3260	0.31087	0.29466	0.30696	0.31531	0.33361	0.34655	0.36299	0.3737
800	0.4961	0.47752	0.45782	0.46233	0.49572	0.52906	0.55889	0.5823	0.60161
1000	0.7015	0.68012	0.6574	0.6798	0.71751	0.77015	0.81704	0.85399	0.88428

These simulation results are carried out by using the Tanner EDA tool. According to these results, optimum delay and power performances are calculated. As far we have studied the simulation results based on 16nm technology node. Now we will study the simulation results based on the 22nm technology node. The propagation delay of multi layer GNR at different interlayer distances for variable interconnect lengths at 22nm technology node is shown in Table 5.3. Figure 5.3 shows the dip at the interlayer distance of 0.5nm. An optimum propagation delay is estimated at this interlayer distance.

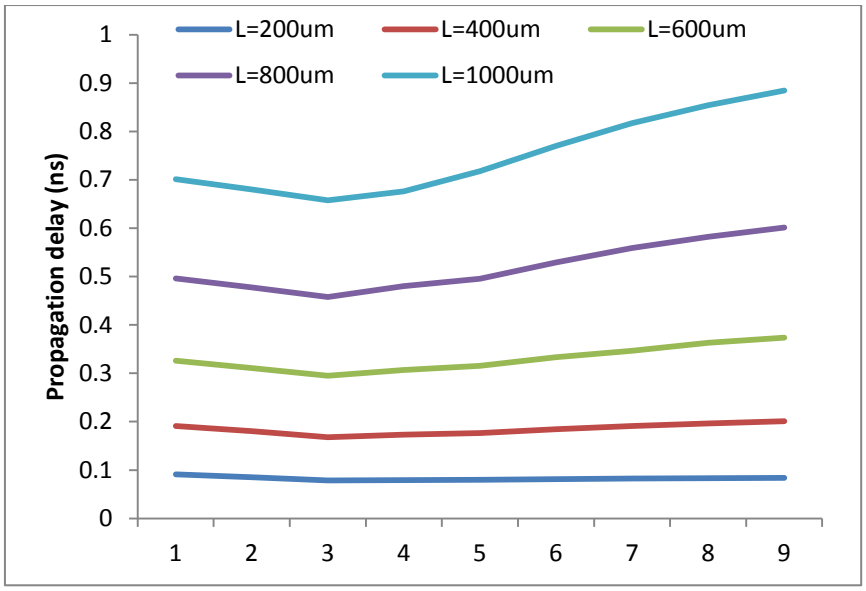

Figure 5.3 Dip showing the optimum interlayer distance of approx. 0.5nm to get the optimum propagation delay of MLGNR at 22nm technology node

Table 5.4 Power Delay Product of MLGNR at different interlayer distances w.r.t Interconnect lengths at 22nm technology node

Length (um)	d=0.34 (nm)	d=0.4 (nm)	d=0.5 (nm)	d=0.55 (nm)	d=0.6 (nm)	d=0.7 (nm)	d=0.8 (nm)	d=0.9 (nm)	d=1 (nm)
200	0.1032	0.096	0.0881	0.0891	0.08970	0.0912	0.0927	0.0935	0.0945
400	0.2252	0.210	0.1950	0.2009	0.20491	0.2137	0.2218	0.2263	0.2333
600	0.4148	0.377	0.3542	0.3695	0.37994	0.4028	0.4187	0.4397	0.4532
800	0.6374	0.606	0.5738	0.6040	0.62472	0.6699	0.7107	0.7427	0.7693
1000	0.9477	0.906	0.8638	0.8844	0.93899	1.0292	1.0996	1.1552	1.2014

The Power Delay Product of MLGNR estimated at different interlayer distances for variable interconnect lengths at 22nm technology node is shown in Table 5.4. Figure 5.4 shows the dip at the interlayer distance of 0.5nm. An optimum value of PDP is estimated at this interlayer distance. The decrease in propagation delay and PDP is observed at 22nm technology node in comparison to 16nm technology node.

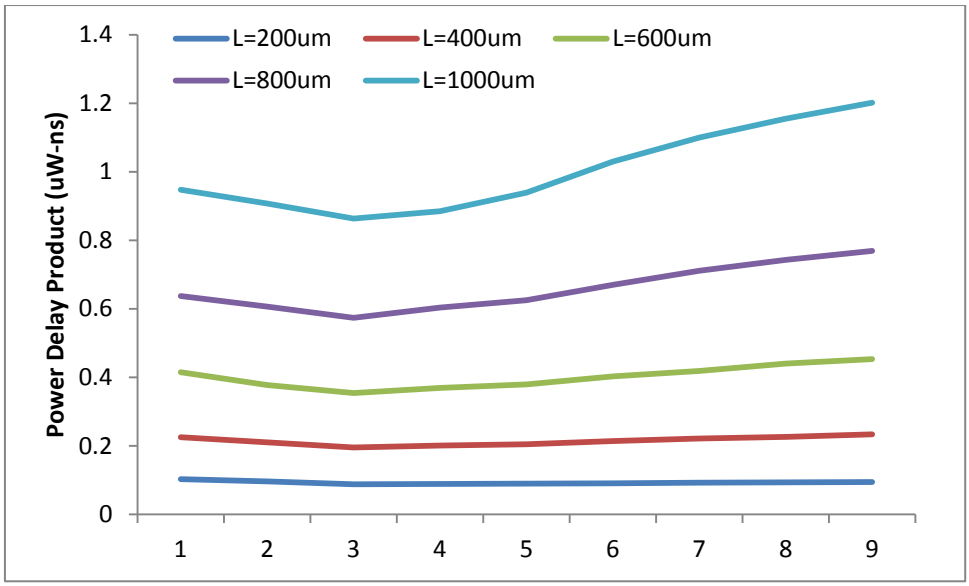

Figure 5.4 Dip showing the optimum interlayer distance of approx. 0.5nm to get the optimum Power Delay Product of MLGNR at 22nm technology node

Table 5.5 Resistance per unit length of different types of GNRs versus width

Width (nm)	Resistance per unit length of mono layer GNR (Ω/um)	Resistance per unit length of Neutral MLGNR (Ω/um)	Resistance per unit length of Doped MLGNR (Ω/um)
10	5421.43	1302	121.07
30	5314	811.4	60.37
50	5302	292	25.31
70	5298	149	12.27
90	5296	90.15	6.84
110	5295	60.35	4.23
130	5294.8	43.21	2.82
150	5294.4	32.45	1.98
170	5294.1	25.26	1.45
190	5293.9	20.22	1.12

Resistance per unit length values as a function of wire width for mono layer GNR, neutral GNR and doped GNR is shown in Table 5.5. Low resistance is reported for doped MLGNR in comparison to the neutral MLGNR and mono layer GNR as shown in Figure 5.5. That's why monolayer GNR is not used because of its high resistance.The specularity is assumed to be negligible in this case.

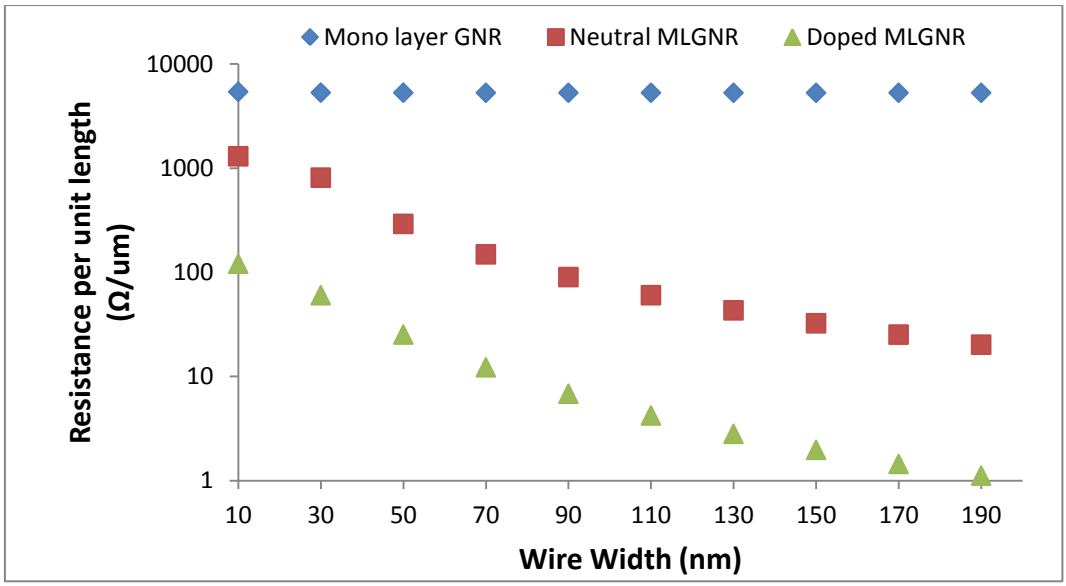

Figure 5.5 Resistance comparison of different types of GNRs. Specularity (p) is assumed to be zero

Table 5.6 Resistance per unit length versus width at different Fermi Energies

Width (nm)	Resistance per unit length at Fermi Energy E_F=0.3eV	Resistance per unit length at Fermi Energy E_F=0.6eV
50	5119	2531
70	2840	1227
90	1689	684
110	1078	423
130	731	282
150	519	198
170	384	145
190	293	110

The conductance of MLGNR is greatly affected by the fermi level. The increase in fermi energy increases the conductance of MLGNR interconnects. Table 5.6 shows the Resistance per unit length values as a function of width at different fermi energies. The fermi level of 0.3eV and 0.6eV is used in this analysis. The fermi level of 0.6eV produces large conductance in comparison to the fermi level of 0.3eV as shown in Figure 5.6.

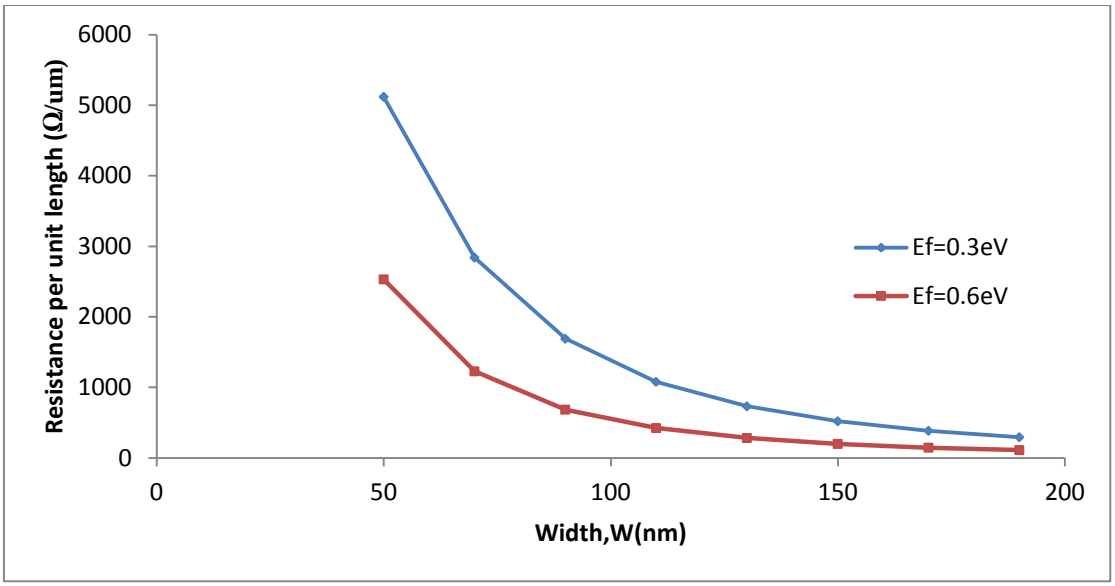

Figure 5.6 Per unit length Resistance values of GNR versus width for lengths larger than mean free path.

Table 5.7 Propagation Delay of MLGNR at different interconnect lengths at 16nm technology node

Length of interconnect (um)	Propagation Delay(ns) E_F = 0.6eV	Propagation Delay(ns) E_F = 0.21eV
100	0.049	0.132
200	0.104	0.186
300	0.182	0.35
400	0.283	0.57
500	0.406	0.82
600	0.551	1.15
700	0.718	1.53
800	0.893	1.96
900	1.118	2.43
1000	1.35	2.9

Propagation delay of MLGNR interconnect for variable interconnect lengths at 16nm technology node is shown in Table 5.7. Results are obtained at different technology nodes. ITRS 2013 parameters are used to calculate the RLC parameters. Simulation results shows that as the fermi level increases, the performance of MLGNR interconnect also increases. The propagation delay decreases on increasing on the fermi level as shown in Figure 5.7.

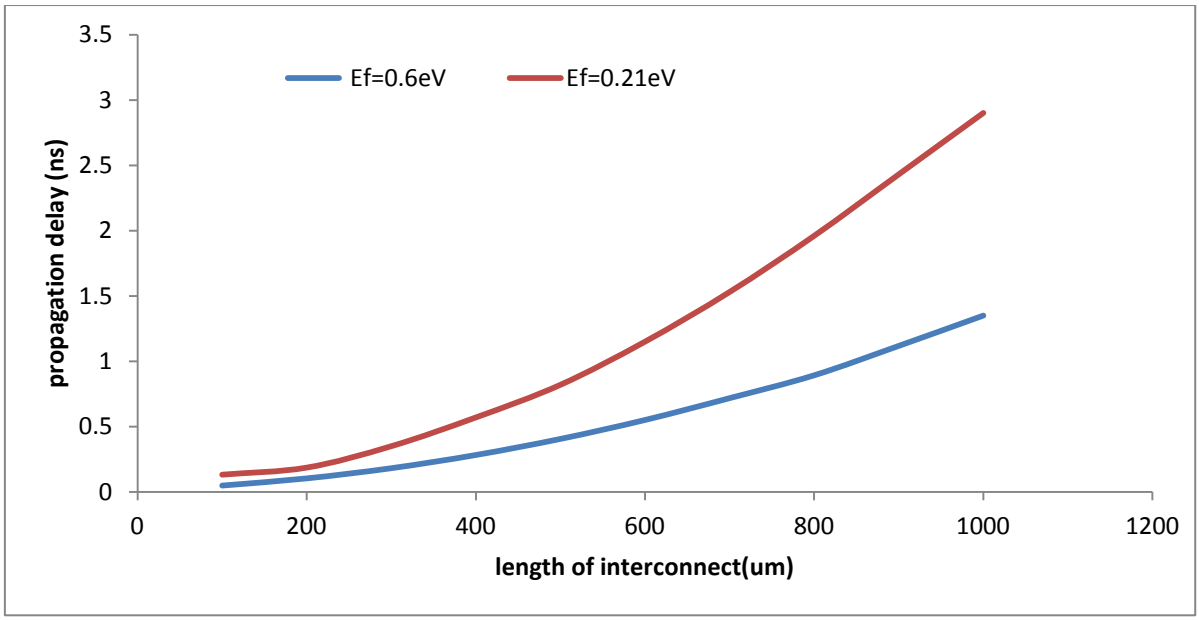

Figure 5.7 Propagation delay of MLGNR versus interconnect length at 16nm technology node

Table 5.8 Power Dissipation of MLGNR at different interconnect lengths at 16nm technology node

Length of interconnect (um)	Power Dissipation (uW) E_F = 0.6eV	Power Dissipation (uW) E_F = 0.21Ev
100	5.31207	6.02
200	5.3164	6.09
300	5.840	6.11
400	6.0691	6.167
500	6.1125	6.258
600	6.1663	6.377
700	6.2263	6.513
800	6.290	6.663
900	6.3695	6.831
1000	6.4555	7.02

Table 5.8 shows the power dissipation of MLGNR at different interconnect lengths at 16nm technology node. The performance of MLGNR increases on increasing the fermi level. The power dissipation increases as the length of interconnect increases as shown in Figure 5.8.

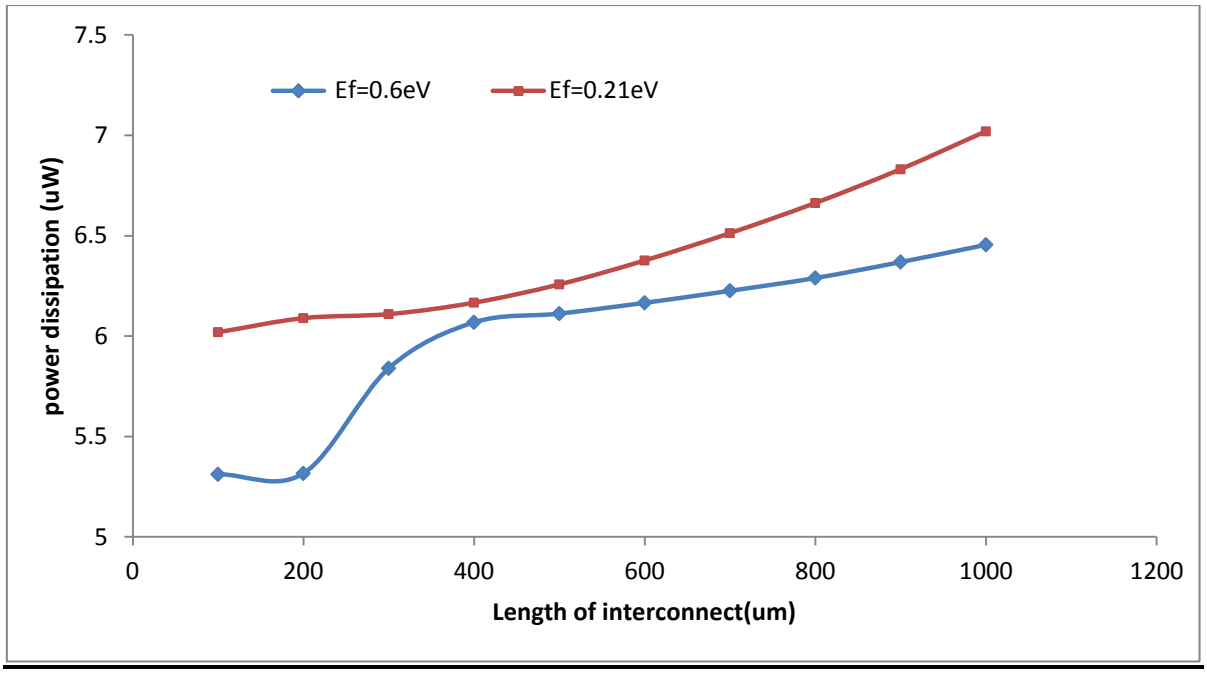

Figure 5.8 Power Dissipation of MLGNR versus interconnect length at 16nm technology node

Table 5.9 Power Delay Product of MLGNR at different interconnect lengths at 16nm technology node

Length of interconnect (um)	Power Delay product (uW-ns) E_F = 0.6eV	Power Delay Product (uW-ns) E_F = 0.21eV
100	0.21248	0.794
200	0.5529	1.132
300	1.0628	2.138
400	1.7175	3.515
500	2.4816	5.131
600	3.3976	7.333
700	4.4704	9.960
800	5.6190	13.05
900	7.1211	16.59
1000	8.7149	20.35

PDP increases with the increase in interconnect length. Table 5.9 shows the PDP of MLGNR at 16nm technology node. As the length of interconnect increases, the percentage difference between different fermi level also increases. The PDP variation between different doped MLGNR is shown in Figure 5.9.

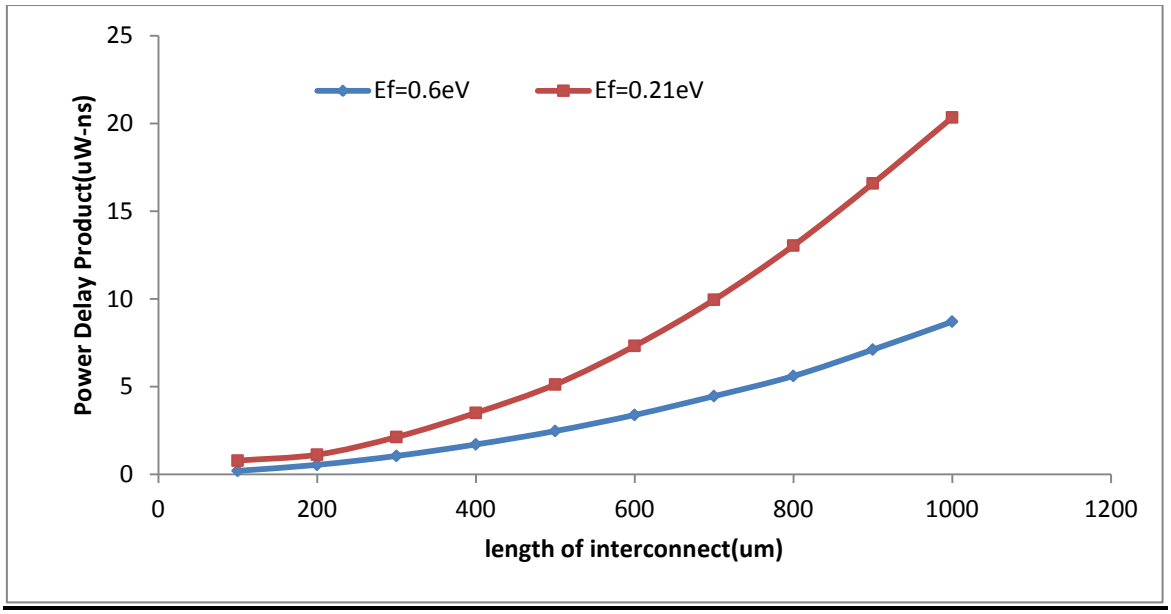

Figure 5.9 Power Delay Product of MLGNR versus interconnect length at 16nm technology node

Table 5.10 Propagation delay of MLGNR at different interconnect lengths at 22nm technology node

Length of interconnect (um)	Propagation Delay(ns) E_F = 0.6eV	Propagation Delay(ns) E_F = 0.21eV
100	0.048	0.129
200	0.08	0.174
300	0.12	0.29
400	0.167	0.43
500	0.221	0.56
600	0.284	0.77
700	0.35	1.05
800	0.43	1.36
900	0.51	1.72
1000	0.6	1.98

The similar analysis is performed on 22nm technology node. It is observed from the table 5.10, as the technology node increases, the propagation delay of interconnect decreases. The doping effect causes reduction in parasitic components and increase in MFP resulting in improved performance of MLGNR at global level as shown in Figure 5.10.

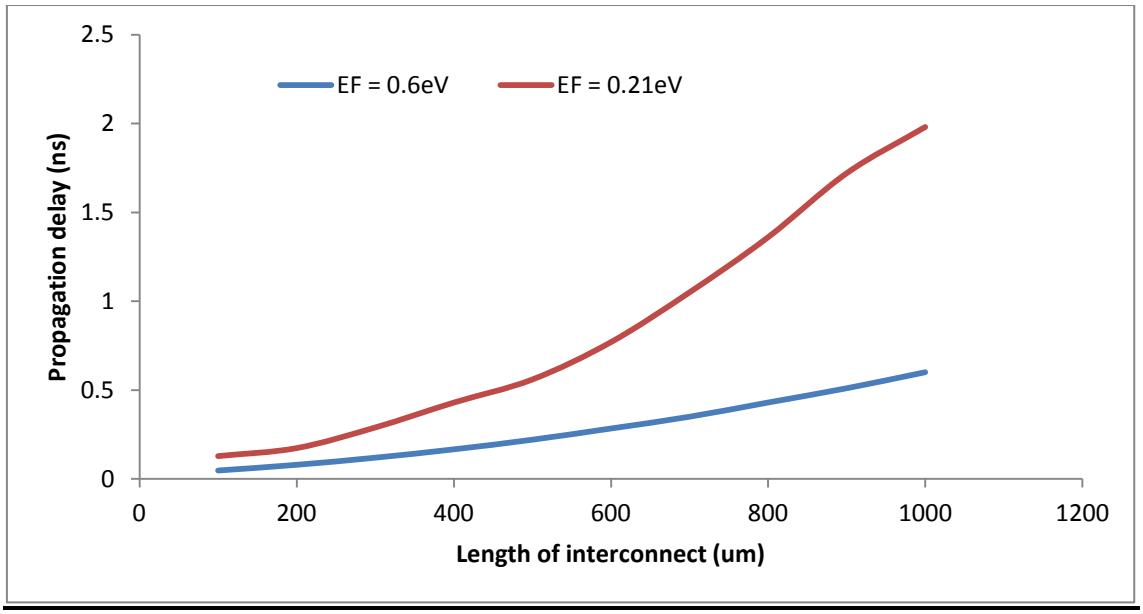

Figure 5.10 Propagation delay of MLGNR versus interconnect length at 22nm technology node

Table 5.11 Power Dissipation of MLGNR at different interconnect lengths at 22nm technology node

Length of interconnect (um)	Power Dissipation (uW) E_F = 0.6eV	Power Dissipation (uW) E_F = 0.21eV
100	1.116	1.224
200	1.134	1.211
300	1.153	1.256
400	1.707	1.288
500	1.1926	1.31
600	1.216	1.395
700	1.241	1.477
800	1.270	1.616
900	1.298	1.78
1000	1.329	2.11

The power dissipation of MLGNR increases on increasing the interconnect length. The effect of different fermi energies on power dissipation of MLGNR is shown in Figure 5.11.

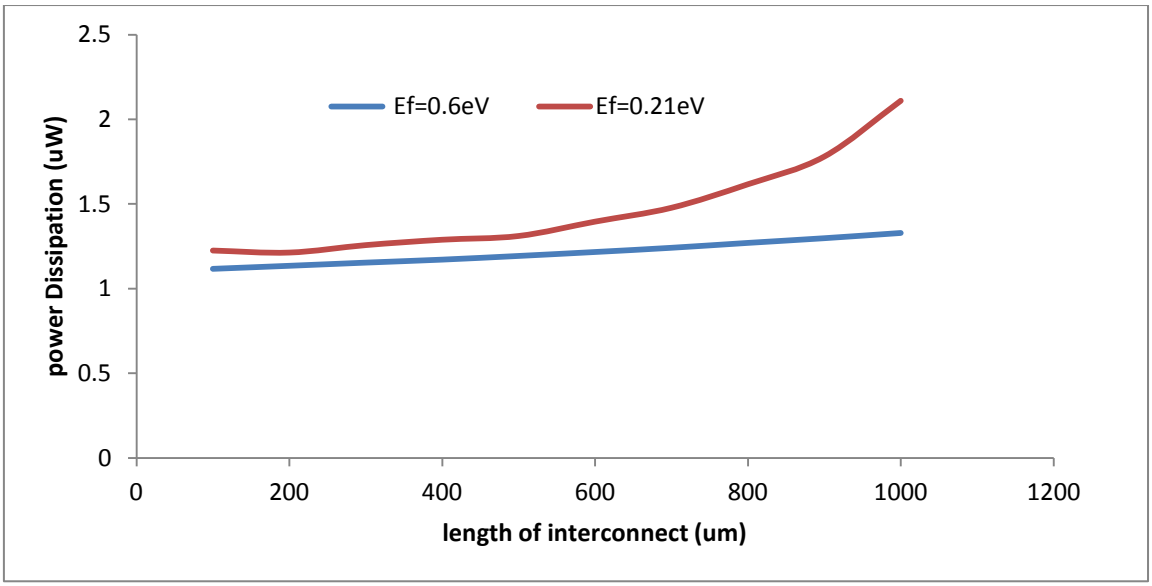

Figure 5.11 Power Dissipation of MLGNR versus interconnect length at 22nm technology node

Table 5.12 Power Delay Product of MLGNR at different interconnect lengths at 22nm technology node

Length of interconnect (um)	Power Delay product (uW-ns) E_F = 0.6eV	Power Delay Product (uW-ns) E_F = 0.21eV
100	0.053	0.157
200	0.09	0.21
300	0.138	0.364
400	0.195	0.553
500	0.263	0.733
600	0.343	1.074
700	0.434	1.550
800	0.546	2.197
900	0.661	3.061
1000	0.797	4.177

Table 5.12 shows the PDP of MLGNR interconnect at 22nm technology node. As the length of interconnect increases, the percentage differences between fermi level increases. It is observed that the impact of fermi energy on power is very small and is almost similar, so the power delay product increases almost similarly as compared with propagation delay as shown in Figure 5.12.

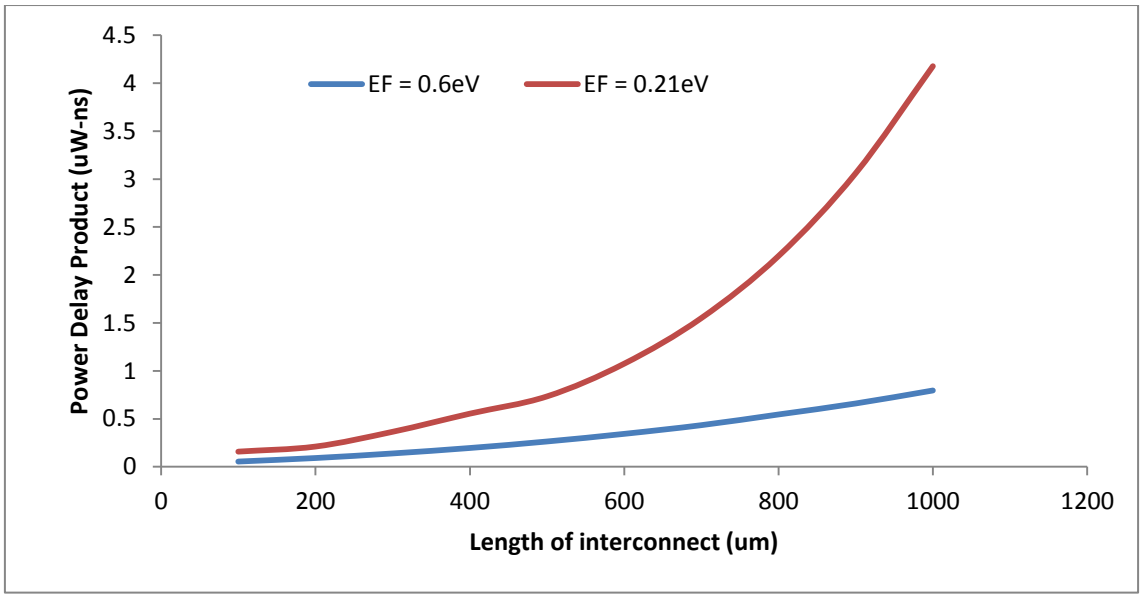

Figure 5.12 Power Delay Product of MLGNR versus interconnect length at 22nm technology node

Table 5.13 Propagation Delay Ratio of MLGNR at different interconnect lengths

Length of interconnect (um)	Propagation Delay (ns) E_F = 0.6eV	Propagation Delay (ns) E_F = 0.21eV
100	0.97	1.07
200	0.76	0.83
300	0.65	0.78
400	0.59	0.68
500	0.54	0.64
600	0.51	0.62
700	0.487	0.577
800	0.481	0.562
900	0.456	0.558
1000	0.444	0.543

Propagation delay ratio of MLGNR interconnect at different interconnect lengths is shown in Table 5.13. With the increase in interconnect length, the propagation delay ratio reduces as shown in Figure 5.13. This is due to the fact that the impedance components of GNR are not strongly dependent on length of interconnect.

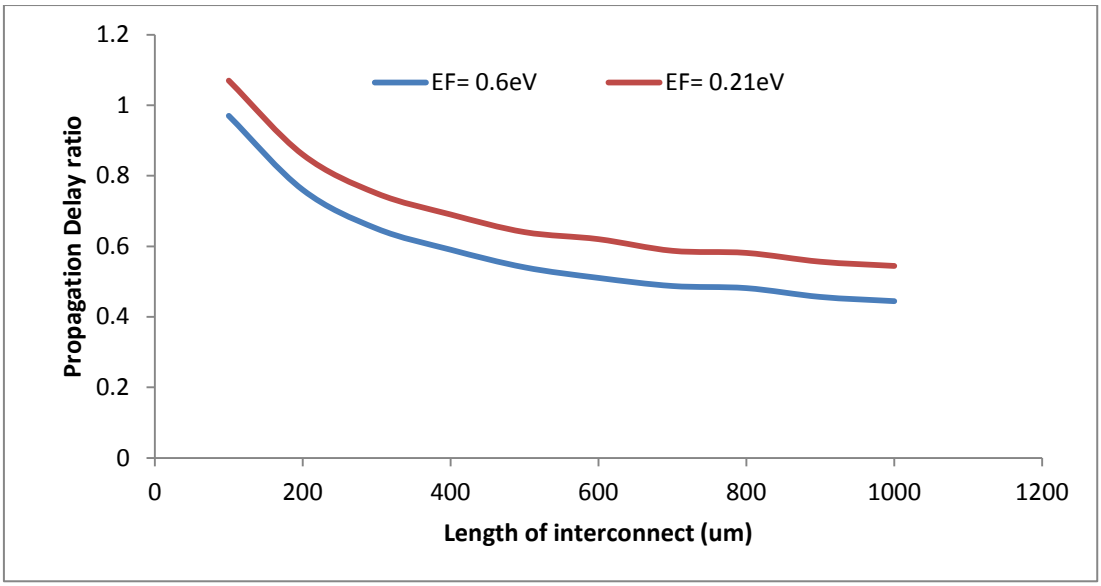

Figure 5.13 Propagation delay ratio of MLGNR versus interconnect length

Table 5.14 Power Delay Product ratio of MLGNR at different interconnect lengths

Length of interconnect (um)	Power Delay product (uW-ns) E_F = 0.6eV	Power Delay Product (uW-ns) E_F = 0.21eV
100	0.25	0.294
200	0.162	0.197
300	0.13	0.16
400	0.113	0.138
500	0.106	0.129
600	0.101	0.123
700	0.097	0.121
800	0.0961	0.116
900	0.0928	0.1128
1000	0.0914	0.1114

Table 5.14 shows the PDP ratio of MLGNR at different interconnect lengths. The Power Delay Product comparison of 16nm and 22nm technology nodes of MLGNR is performed. The propagation delay ratio reduces with the increase in interconnect length as shown in Figure 5.14.

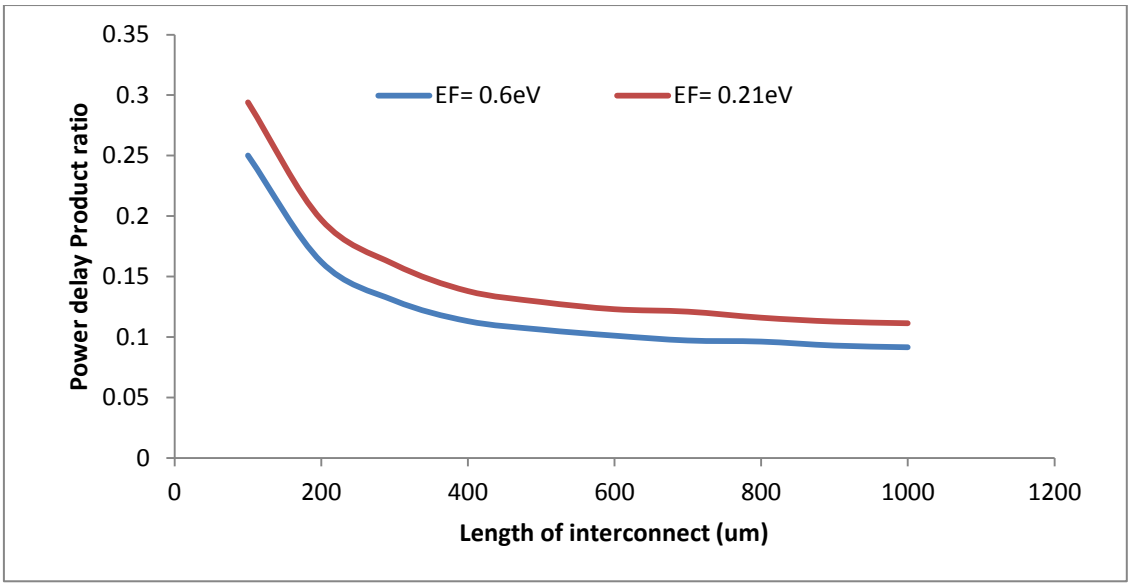

Figure 5.14 Power Delay Product ratio of MLGNR at different interconnect lengths

Intercalation doping affects the performance of multi layer GNR. The propagation delay and power dissipation reduces on increasing the fermi energy. As the scaling continues the delay as well as power of MLGNR increases. For narrow metallic GNRs (< 20nm) with diffusive edge scattering, there is no effect of fermi energy on conductance because of shorter mean free path of additional conducting modes. Wide semiconductor and metallic GNRs (> 100nm) have similar conductances Narrow semiconductor GNRs have high resistances. For a doped multi layer GNR, the optimum interlayer distance is around 0.5nm at which the MLGNR provides the optimum propagation delay, power dissipation and PDP.

CHAPTER 6
CONCLUSION AND FUTURE SCOPE

6.1 Conclusion

In this dissertation, Propagation delay and power dissipation are compared by varying the interlayer distance for various technology nodes such as 16nm and 22nm by using the TANNER EDA Tool. According to the simulation results, the optimum delay and power performances are calculated. Based on these performances, an optimum value of interlayer distance is proposed which is approximately 0.5nm for a doped MLGNR. Therefore MLGNR with optimum interlayer distance can be predicted as the future of global VLSI interconnects.

The performance of multi layer GNR is also analyzed. The propagation delay, power dissipation and power delay product of MLGNR is also calculated by varying doping. It is observed that propagation delay and power dissipation of MLGNR interconnect reduces on increasing the fermi energy. The impedance parameters at 16nm and 22nm are calculated and are then used to simulate the delay and power dissipation. ITRS 2013 simulation parameters are used for calculation of impedance parameters for all the technology nodes. The variation in performance of MLGNR is observed with the scaling of technology nodes.

The conductance of GNR is also calculated as a function of width, chirality and fermi energy. The conductance increases on increasing the fermi level. Monolayer, Neutral multilayer and doped multilayer Zigzag GNR interconnects are analyzed from conductance perspectives.

6.2 Future Scope

The fabrication issues of Multilayer Graphene nano ribbon are needed to be addressed and more effective fabrication techniques of GNR are also needed to be studied and developed in order to increase the performance of GNR interconnect. The influence of temperature on the performance of GNR is required to be studied in future. The work presented in this report is at 22nm and 16nm technology nodes and this can be further extended to 10nm technology node.

REFERENCES

[1]. K. C. Saraswat and F. Mohammadi, "Effect of scaling of interconnects on the time delay of VLSI circuits," *IEEE Journal of Solid-State Circuits*, vol. 17, no. 2, pp. 275-280, 1982.

[2]. International Technology Roadmap for Semiconductors (ITRS-2013) reports. Available: http://www.itrs2.net/itrs-reports.html.

[3]. T. Ragheb and Y. Massoud, "On the modeling of resistance in graphene nanoribbon (GNR) for future interconnect applications," in *Proc. of the IEEE/ACM International. Conference on Computer-Aided Design*, pp. 593–597, 2008.

[4]. V. R. Kumar, M. K. Majumder, N. R. Kukkam, and B. K. Kaushik, "Time and frequency domain analysis of MLGNR interconnects," *IEEE Transactions on Nanotechnology*, vol. 14, no. 3, pp. 484–492, 2015.

[5]. Atul K. Nishad and Rohit Sharma, "Analytical Time Domain Models for Performance Optimization of MLGNR Interconnects," in *Proc. of the IEEE International Interconnect Technology Conference*, pp. 231–234, 2009.

[6]. R. Murali, K. Brenner, Y. Yang, T. Beck, and J. D. Meindl, "Resistivity of graphene Nano ribbon interconnects," *IEEE Electron Device Letters*, vol. 30, no. 6, pp. 611–613, 2009.

[7]. C. Xu, H. Li, and K. Banerjee, "Graphene nano-ribbon (GNR) interconnects: A genuine contender or a delusive dream?," in *Proc. of the IEEE International Electron Device Meeting*, pp. 201–204, 2008.

[8]. A. K. Nishad and R. Verma, "Performance improvement in SC-MLGNRs interconnects using interlayer dielectric insertion," *IEEE Transactions on Emerging Topics in Computing*, vol. 3, no. 4, pp. 470–482, 2015.

[9]. A. Maffucci and G. Miano, "Number of conducting channels for armchair and zig-zag graphene nanoribbon interconnects," *IEEE Transactions on Nanotechnology*, vol. 12, no. 5, pp. 817–823, 2013.

[10]. W.-S. Zhao and W.-Y. Yin, "Comparative study on multilayer graphene nanoribbon (MLGNR) interconnects," *IEEE Transactions on Electromagnetic Compatibility*, vol. 56,

[11]. C. Xu, H. Li, and K. Banerjee "Signal Integrity Analysis of Graphene Nano Ribbon Interconnects", *Electronic Properties Of Carbon Nanotubes*, Intechopen, pp. 475–494, 2011.

[12]. C. Xu, H. Li, and K. Banerjee, "Modeling, analysis, and design of graphene nanoribbons interconnects," *IEEE Transactions on Electron Devices,* vol. 56, no. 8, pp 1567–1578, 2009.

[13]. H. Li, C. Xu, N. Srivastava, and K. Banerjee, "Carbon nano materials for next generation interconnects and passives: physics, status, and prospects," *IEEE Transactions on Electron* Devices, vol. 56, no. 9, pp. 1799–1821, 2009.

[14]. A. Naeemi and J. D. Meindl, "Conductance modeling for graphene nanoribbon (GNR interconnects," *IEEE Electron Device Letters*, vol. 28, no. 5, pp. 428–431, 2007.

[15]. Karmjit Singh, and Balwinder Raj," Temperature-Dependent Modeling and Performance Evaluation of Multi-Walled CNT and Single Walled CNT as Global Interconnects," Journal of Electronic Materials 44, no. 12 (2015): 4825-4835.

[16]. Karmjit Singh, and Balwinder Raj," Performance and analysis of temperature dependent multi walled CNTs as global interconnects at different technology nodes,"Journal of Computational Electronics14, no.2 (2015): 469-476.

[17]. Karmjit Singh, and Balwinder Raj," Influence of temperature on MWCNT bundle, SWCNT bundle and copper interconnects for nano scaled technology nodes."Journal of Materials Science: Materials in Electronics26,no. 8(2015):6134-6142.

[18]. A. Naeemi and J. D. Meindl, "Compact physics-based circuit models for graphene Nano ribbon interconnects," *IEEE Transactions on Electron Devices*, vol. 56, no. pp. 1822– 1833, 2009. no. 3, pp. 638–645, 2014.

[19]. Predictive Technology Model (PTM). Available: http://ptm.asu.edu/.

[20]. G. Lupina, M. Lukosius, J. Kitzmann, J. Dabrowski, A. Wolff, and W. Mehr "Performance and Energy per bit modeling of MLGNR conductors, *Applied Physics Letters*, vol. 103, no. 18, pp. 183116-1–183116-4, 2013.

[21]. W.-K. Tse, E. H. Hwang, and S. D. Sarma, "Ballistic hot electron transport in graphene," *Applied Physics Letters*, vol. 93, no. 2, pp. 023128-1–023128-3, 2008.

[22]. B. K. Kaushik, M. K. Majumder, and V. Ramesh Kumar, "Comparison of propagation delay in single and multi layer GNR interconnects," *IEEE Circuits and Systems Magazine*, vol. 14, no. 4, pp. 16–35, 2014

[23]. P. J. Burke, "Luttinger liquid theory as a model of the gigahertz electrical properties of carbon nanotubes," *IEEE Transactions on Nanotechnology*, vol. 1, no. 3, pp. 129–144, 2002.

[24]. T. Ando, "Screening effect and impurity scattering in monolayer graphene," *Journal of the Physical Society of Japan*, vol. 75, no. 7, pp. 074716-1–074716-7, 2006.

[25]. S. Adam, E. H. Hwang, V. M. Galitski, and S. D. Sarma, "A self-consistent theory for graphene transport," in *Proc. of the National Academy of Sciences of the United States of America*, vol. 104, no. 47, pp. 18392–18397, 2007.

[26]. Azad Naeemi and James D., "Performance Benchmarking for Graphene nano ribbon, carbon nano tube and copper interconnect *Journal of Computational Electronics*, vol. 14, no. 2, pp. 469–476, 2015.

[27]. Predictive Technology Model (PTM). Available: http://ptm.asu.edu/.

[28]. A. A. Balandin, S. Ghosh, W. Bao, I. Calizo, D. Teweldebrhan, F. Miao, and C. N. Lau, "Superior thermal conductivity of single-layer graphene," *Nano Letters*, vol. 8, no. 3, pp. 902–907, 2008.

[29]. Narasihma Reddy, Manoj Kumar and B.K. Kaushik "Optimized Delay and Power Performances in Multilayer Graphene nano Ribbon Interconnects," *Journal of Materials Science: Materials in Electronics*, vol. 26, no. 8, pp. 6134–6142, 2015.

[30]. K. Hosono and K. Wakabayashi, "Dielectric environment effect on carrier mobility of graphene double-layer structure," *Applied Physics Letters*, vol. 103, no. 3, pp. 033102-1–033102-4, 2013.

[31]. C. R. Dean, A. F. Young, I. Meric, C. Lee, L. Wang, S. Sorgenfrei, K. Watanabe, T. Taniguchi, P. Kim, K. L. Shepard, and J. Hone, "Boron nitride substrates for highquality graphene electronics," *Nature Nanotechnology*, vol. 5, pp. 722–726, 2010.

[32]. C. Xu, H. Li, and K. Banerjee, "Signal transmission analysis of Multilayer Graphene nano ribbon interconnects," *IEEE Transactions Electron Devices*, vol. 50, no. 4, pp. 1094–1102, 2003.

[33]. Vachan Kumar and Azad Naemmi, "Review of Multilayer Graphene Nano ribbon for On Chip interconnect Applications," *Nano Letters*, vol. 8, no. 7, pp. 1912–1915, 2008.

[34]. Y. Fang, W. S. Zhao, X. Wang, F. Jiang, and W. Y. Yin, "Circuit modeling of multilayer graphene nanoribbon (MLGNR) interconnects," in *Proc. of the Asia Pacific Symposium on Electromagnetic Compatibility*, pp. 625–628, 2012.

[35]. S. H. Nasiri, R. Faez, and M. K. Moravvej-Farshi, "Stability analysis in Graphene nano ribbon interconnects," *Modern Physics Letters B*, vol. 26, no. 1, pp. 1150004-1–1150004-5, 2011.

[36]. W.-S. Zhao and W.-Y. Yin, "Comparative study on multilayer graphene nanoribbon (MLGNR) interconnects," *IEEE Transactions on Electromagnetic Compatibility*, vol. 56,no.4.

[37]. N. Srivastava and K. Banerjee, "Interconnect challenges for nanoscale electronic circuits," *The Journal of The Minerals, Metals & Materials Society*, vol. 56, no. 10, pp. 30–31, 2004.

[38]. R. Murali, Y. Yang, K. Brenner, T. Beck, and J. D. Meindl, "Breakdown current density of graphene nanoribbons," *Applied Physics Letters*, vol. 94, no. 24, pp. 243114-1–243114-3, 2009.

[39]. A. H. C. Neto, F. Guinea, N. M. R. Peres, K. S. Novoselov, and A. K. Geim, "The electronic properties of graphene," *Reviews of Modern Physics*, vol. 81, no. 1, pp. 109–162, 2009.

[40]. T. Yu, C.-W. Liang, C. Kim, E.-S. Song, and B. Yu, "Three-dimensional stacked multilayer graphene interconnects," *IEEE Electron Device Letters*, vol. 32, no. 8, pp. 1110–1112, 2011.

[41]. A. Ceyhan and A. Naeemi, "Cu interconnect limitations and opportunities for SWNT interconnects at the end of the roadmap," *IEEE Transactions on Electron Devices*, vol. 60, no. 1, pp. 374–382, 2012.

[42]. Yash Agrawal, Rajeevan Chandel, M.G Kumar, "Performance Analysis of Multilayer Graphene Nanoribbon in current Mode Signalling System, *Transactions on Electromagnetic Compatibility*, vol. 56,no.4, pp.30-31,2004.

[43]. Mayank Kumar Rai, A.K Chaterjee, Sankar Sarkar, B.K Kaushik, "Performance Analysis of Multilayer Graphene Nanoribbon (MLGNR) Interconnects,"

[44]. S. Adam, E. H. Hwang, V. M. Galitski, and S. D. Sarma, "A self-consistent theory for graphene transport," in *Proc. of the National Academy of Sciences of the United States of America*, vol. 104, no. 47, pp. 18392–18397, 2007.

[45]. W.-K. Tse, E. H. Hwang, and S. D. Sarma, "Ballistic hot electron transport in graphene," *Applied Physics Letters*, vol. 93, no. 2, pp. 023128-1–023128-3, 2008.

Turnitin Originality Report

601562014 by Kashish Wadhwa

From xyz (kss)

Processed on 17-Jul-2017 16:15 IST
ID: 831345705
Word Count: 14201

Similarity Index	Similarity by Source	
17%	Internet Sources:	6%
	Publications:	13%
	Student Papers:	2%

sources:

1 3% match (publications)
Zhao, Wen-Sheng, and Wen-Yan Yin. "Comparative Study on Multilayer Graphene Nanoribbon (MLGNR) Interconnects", IEEE Transactions on Electromagnetic Compatibility, 2014.

2 2% match (publications)
Kumar, Gaurav, and Gargi Khanna. "Propagation delay comparison of single and Multi-layer graphene nano ribbon interconnects using equivalent single-conductor (ESC) model", 2015 International Conference on Computation of Power Energy Information and Communication (ICCPEIC), 2015.

3 2% match (publications)
Rai, Mayank Kumar, Ashoke Kumar Chatterjee, Sankar Sarkar, and B. K. Kaushik. "Performance analysis of multilayer graphene nanoribbon (MLGNR) interconnects", Journal of Computational Electronics, 2016.

4 1% match (Internet from 16-Nov-2006)
http://www.sal.hut.fi/Publications/pdf-files/tmur98.pdf

5 1% match (Internet from 11-Oct-2010)
http://www.ece.ucsb.edu/Faculty/Banerjee/pubs/TED_2009_GNR.pdf

6 1% match (publications)
Kumar, Vobulapuram Ramesh, Manoj Kumar Majumder, Narasimha Reddy Kukkam, and Brajesh Kumar Kaushik. "Time and Frequency Domain Analysis of MLGNR Interconnects", IEEE Transactions on Nanotechnology, 2015.

7 1% match (publications)
Nishad, Atul, and Rohit Sharma. "Performance Improvement in SC-MLGNRs Interconnects using Interlayer Dielectric Insertion", IEEE Transactions on Emerging Topics in Computing, 2015.

8 1% match (publications)
Reddy, K. Narasimha, Manoj Kumar Majumder, B. K. Kaushik, B. Anand, and Pankaj Kumar Das. "Optimized delay and power performances in multilayer graphene nanoribbon interconnects", 2012 Asia Pacific Conference on Postgraduate Research in Microelectronics and Electronics, 2012.

9 1% match (publications)
SpringerBriefs in Applied Sciences and Technology, 2016.

10 < 1% match (Internet from 29-Apr-2012)
http://dspace.thapar.edu:8080/dspace/bitstream/10266/757/1/satyarth_thesis1.pdf

11 < 1% match (publications)
Sharda, Vangmayee, and R. P. Agarwal. "Review of Graphene Nanoribbons", 2014 Recent Advances in Engineering and Computational Sciences (RAECS), 2014.

< 1% match (Internet from 16-Feb-2017)

12 http://documents.mx/download/link/ramirez-dis

13 < 1% match (Internet from 29-Apr-2012)
http://dspace.thapar.edu:8080/dspace/bitstream/10266/790/1/Analysing+and+Visualizing+the+effect+of+noise+on+Compressed+

14 < 1% match (Internet from 22-Dec-2012)
http://dspace.thapar.edu:8080/dspace/bitstream/10266/1767/1/chetan_thesis.pdf

15 < 1% match (Internet from 23-Jul-2012)
http://dspace.thapar.edu:8080/dspace/bitstream/123456789/138/1/6040407.pdf

16 < 1% match (Internet from 20-Apr-2012)
http://gdeepak.com/thesisme/Thesis%20Complexity%20Analysis%20Involving%20Heterogeneous%20System.pdf

17 < 1% match (Internet from 20-Apr-2012)
http://gdeepak.com/thesisme/Choosing%20Best%20Hashing%20Strategies%20and%20hash%20functions.pdf

18 < 1% match (publications)
Journal of Engineering, Design and Technology, Volume 11, Issue 1 (2013-05-27)

19 < 1% match (publications)
Cui, Jiang-Peng, Wen-Sheng Zhao, Wen-Yan Yin, and Jun Hu. "Signal Transmission Analysis of Multilayer Graphene Nano-Ribbon (MLGNR) Interconnects", IEEE Transactions on Electromagnetic Compatibility, 2012.

20 < 1% match (Internet from 12-May-2013)
http://www.scribd.com/doc/70966063/290/FIGURE-8-26?sh=586b7977076836bf

21 < 1% match (publications)
Journal of Engineering, Design and Technology, Volume 8, Issue 3 (2010-11-01)

22 < 1% match (Internet from 20-Apr-2014)
http://ninf.apgrid.org/papers/hpdc01takefusa/hpdc2001-takefusa.pdf

23 < 1% match (publications)
Majumder, Manoj Kumar, B. K. Kaushik, K. Narasimha Reddy, and S. K. Manhas. "Comparison of propagation delay in single- and multi-layer graphene nanoribbon interconnects", 2012 5th International Conference on Computers and Devices for Communication (CODEC), 2012.

24 < 1% match (Internet from 31-Oct-2010)
http://www.sese.uwa.edu.au/__data/page/96394/crawford_2003.pdf

25 < 1% match (Internet from 31-Oct-2012)
http://fairchildsemi.com.tw/ds/HC/HCPL0611.pdf

26 < 1% match (Internet from 23-Jul-2012)
http://dspace.thapar.edu:8080/dspace/bitstream/123456789/181/1/8044102.pdf

27 < 1% match (Internet from 22-Dec-2012)
http://dspace.thapar.edu:8080/dspace/bitstream/10266/1764/1/abhinav.pdf